


5-2017

# A Genetic Analysis of Nuclear Functions of the Lipin Protein in *Drosophila melanogaster*

Xeniya Rudolf

*University of Arkansas, Fayetteville*

Follow this and additional works at: <http://scholarworks.uark.edu/etd>

 Part of the [Biochemistry Commons](#), [Molecular Biology Commons](#), and the [Molecular Genetics Commons](#)

---

## Recommended Citation

Rudolf, Xeniya, "A Genetic Analysis of Nuclear Functions of the Lipin Protein in *Drosophila melanogaster*" (2017). *Theses and Dissertations*. 2011.

<http://scholarworks.uark.edu/etd/2011>

This Thesis is brought to you for free and open access by ScholarWorks@UARK. It has been accepted for inclusion in Theses and Dissertations by an authorized administrator of ScholarWorks@UARK. For more information, please contact [scholar@uark.edu](mailto:scholar@uark.edu), [ccmiddle@uark.edu](mailto:ccmiddle@uark.edu).

A Genetic Analysis of Nuclear Functions of the Lipin Protein in *Drosophila melanogaster*

A thesis submitted in partial fulfillment  
of the requirements for the degree of  
Master of Science in Cell and Molecular Biology

by

Xeniya Valeriyivna Rudolf  
University of Arkansas  
Bachelor of Science in Biology, 2015

May 2017  
University of Arkansas

This thesis is approved for recommendation to the Graduate Council.

---

Dr. Michael Lehmann  
Thesis Director

---

Dr. Tim Evans  
Committee Member

---

Dr. Fiona Goggin  
Committee Member

## **ABSTRACT**

Lipins are a family of proteins that have critical functions in the control of fat storage and energy homeostasis. Biochemically, lipins have two functions. They provide an enzymatic activity (phosphatidate phosphatase or PAP activity) in the glycerol-3 phosphate pathway that leads to the production of storage fats (triacylglycerols). In addition, they play a role in the regulation of genes in the cell nucleus as transcriptional co-regulators. The PAP activity of lipins has been widely studied in a number of organisms. However, the transcriptional co-regulator function is not as well described in the literature. The transcriptional function of lipins depends on its nuclear translocation caused by the presence of a nuclear localization signal (NLS) in the protein. Data from our lab have shown that expression of Lipin protein lacking the NLS (Lipin $\Delta$ NLS) from a transgene leads to a disruption of timely development of *Drosophila melanogaster*. This suggests that Lipin has nuclear roles in the control of development.

The overarching goal of this project was to further examine nuclear roles of Lipin in *Drosophila melanogaster*. Lipin $\Delta$ NLS mutant was generated by CRISPR/Cas9 mutagenesis. Phenotypic and genetic analyses of the Lipin $\Delta$ NLS mutant indicate that nuclear functions of Lipin are essential for animal survival. Lipin $\Delta$ NLS and Lipin $\Delta$ PAP mutants complement each other restoring enzymatic and nuclear functions in these transheterozygous animals. Generation of a Lipin $\Delta$ NLS mutant provides a variety of future directions that can be pursued by our laboratory.

## **ACKNOWLEDGEMENTS**

Special thanks go to the faculty and staff of Biological Sciences Department as well as Cell and Molecular Biology Program.

## TABLE OF CONTENTS

I. INTRODUCTION	1
A. Background	1
B. Lipin Gene Family	1
C. Molecular Functions of Lipin	2
D. Lipins in Mammals	3
E. Use of <i>Drosophila melanogaster</i> in Studying Transcriptional Coactivator Functions of Lipin	5
II. MATERIALS AND METHODS	7
A. Fly Food Preparation	7
B. Cloning of gRNA into pCFD3 Plasmid	8
C. CRISPR/Cas9 Mutagenesis: Run I	12
D. CRISPR/Cas9 Mutagenesis: Run II	14
E. CRISPR/Cas9 Mutagenesis: Run III	15
F. Establishing Stable Stocks	16
G. DNA Extraction from Single Flies	17
H. PCR Test for Mutations: CRISPR/Cas9 Run I	17
I. PCR Test for Mutations: CRISPR/Cas9 Run II	19
J. PCR Test for Mutations: CRISPR/Cas9 Run III	20
K. PCR Purification	20
L. Testing Purified PCR Sample Concentrations by Gel Electrophoresis	21
M. Sending Samples for Sequencing	22
N. Determining if Mutant Stocks Produced Homozygous Animals at Any Life Stages	22
O. Analyzing Viability of Lipin Mutants and Determining Lethal Phase	22
P. Western Blot Analysis of CRISPR/Cas9 Mutants	23
Q. Whole Gene Sequencing of Lipin $\Delta$ NLS Mutant	26
R. Expression of Lipin $\Delta$ NLS or RNAi of Lipin in Malpighian Tubules	28
S. Immunostaining of Lipin in Malpighian Tubules and Fat Bodies	30
T. Expression of Lipin $\Delta$ NLS in the Ring Gland	31
III. RESULTS	33

<b>A. Using CRISPR/Cas9 to Generate a Lipin<math>\Delta</math>NLS Mutant</b>	33
<b>B. Lipin<math>\Delta</math>NLS Identification</b>	36
<b>C. Testing Lipin<math>\Delta</math>NLS Mutant for Presence of Secondary Mutations</b>	37
<b>D. Genetic Complementation between Lipin<math>\Delta</math>NLS and Lipin<math>\Delta</math>PAP</b>	40
<b>E. Characterization of Non-<math>\Delta</math>NLS Mutant <i>Lipin</i> Alleles Created by CRISPR/Cas9 Mutagenesis</b>	42
<b>F. Analysis of CRISPR/Cas9 Mutagenized Animals for Secondary Mutations</b>	42
<b>G. Testing Mutant Animals for Predicted Lipin Protein Product Sizes</b>	44
<b>H. Function of Lipin in Malpighian Tubules</b>	48
<b>I. Overexpression of Lipin<math>\Delta</math>NLS in the Ring Gland</b>	52
<b>IV. DISCUSSION</b>	54
<b>V. REFERENCES</b>	58
<b>VI. APPENDIX: NUCLEOTIDE AND AMINO ACID ALIGNMENTS OF CRISPR/CAS GENERATED MUTANTS</b>	62
<b>A. LipinNLS+6(+2)FS285</b>	62
<b>B. LipinNLS_IF276<math>\Delta</math>K</b>	63
<b>C. LipinNLS_IF273<math>\Delta</math>KTK</b>	64
<b>D. LipinNLS<math>\Delta</math>1FS284</b>	65
<b>E. LipinNLS+2<math>\Delta</math>1FS284</b>	66
<b>F. LipinNLS<math>\Delta</math>2FS304</b>	67
<b>G. LipinNLS+2<math>\Delta</math>5FS303</b>	68
<b>H. LipinNLS<math>\Delta</math>5FS303</b>	69
<b>I. LipinNLS-3<math>\Delta</math>7FS282</b>	70
<b>J. LipinNLS-6<math>\Delta</math>13FS280</b>	71
<b>K. LipinNLS-47<math>\Delta</math>47(+1)FS269</b>	72

## **I. INTRODUCTION**

### **A. Background**

Diseases such as obesity, insulin resistance, diabetes, dyslipidemia, hypertension, coronary heart disease, and cancer strongly suggest the importance of proper regulation of adipogenesis and fat storage in adipocytes in humans (Garg, 2004; Smyth, 2006). Excessive or reduced levels of triglyceride (TAG) synthesis directly influence modes of lipid accumulation in liver and skeletal muscle.

A random accident in 1981 has led to the discovery of lipin gene family. Jackson Laboratory observed an unusual mouse phenotype (Bar Harbor, Maine). The animals appeared normal after birth, but with time, developed fatty liver and hypertriglyceridemia (Langer et al., 1989). On average, mutant animals maintained 25% lower body weight than normal animals. Mutant animals were given a name fatty liver dystrophy (*fld*) and were characterized as lacking in adipose tissue and insulin resistance (Rue et al., 2000).

Lipin-1 gene was first described in 2001 through cloning experiments in fatty liver dystrophy background (Péterfy et al., 2001).

### **B. Lipin Gene Family**

The family of lipin proteins exists in a variety of species ranging from yeast to humans. Among the different species, lipin proteins have evolutionary conserved regions called NLIP and CLIP domains implying their importance in the function of the proteins. The CLIP domain in mammals, as well as *Drosophila melanogaster* contains the haloacid dehydrogenase motif DXDXT which corresponds to phosphatases (PAP) and the transcription binding motif LXXIL (Han et al., 2006; and Finck\* et al., 2006).

Two of mammalian lipin proteins have been shown to act as transcriptional co-activators in a manner independent from their PAP activity by interaction with proliferator-activated receptor (PPAR)  $\alpha$ , PPAR co-activator-1 $\alpha$  (PGC-1 $\alpha$ ), and PPAR $\gamma$  (Koh et al., 2008; Finck\* et al., 2006; and Donkor et al., 2009).

### **C. Molecular Functions of Lipin**

Lipin has two primary functions within a cell. First, lipin can act as phosphatidate phosphatase (PAP) in a diacylglycerol (DAG) synthesis pathway. This pathway includes a series of steps involving addition of acyl groups to glycerol phosphate. The conversion of phosphatidate to DAG is catalyzed by lipin-1 in mammals. DAG can further be converted into triacylglycerol (TAG) or neutral phospholipids, phosphatidylcholine, and phosphatidylethanolamine (Vance et al., 2004).

The second function is lipin's ability to regulate gene expression through a mechanism involving nuclear entry. Initially, chromatin immunoprecipitation (ChIP) of lipin's homolog in yeast (SMP2) showed proteins association with the promoter region of genes, which code for phospholipid biosynthesis (Santos-Rosa et al., 2005). It was later shown by Finck et al. that mammalian lipin-1 acts as a transcriptional coactivator of fatty acid oxidation genes under caloric restriction conditions (Finck et al., 2006). First, lipin-1 gene expression was shown to be activated by fasting among other factors in PGC-1 $\alpha$  dependent manner (Finck et al., 2006). A gene expression profiling (microarray) was conducted in wild-type mice to evaluate genes highly expressed under starvation conditions, as a result, lipin-1 transcription was observed to be highly induced. However, mice homozygous for PGC-1 $\alpha$  knockout were not able to respond to starvation with activation of lipin-1 gene. Second, overexpression of lipin-1 in mouse



liver using an adenoviral vector (Ad-lipin) showed an effect on increase of transcription of many genes associated with fatty acid uptake and utilization along with nuclear receptor PPAR $\alpha$ ; the Krebs's cycle enzymes; and proteins involved in mitochondrial oxidative phosphorylation (Finck et al., 2006). On the other hand, the expression of genes involved in fatty acid and TAG synthesis showed a decline as a response to lipin-1 overexpression. Third, Glutathione S-transferase (GST) pulldown assay showed physical interaction of PPAR $\alpha$  with the LXXIL motif of lipin-1 indicating that nuclear functions of lipin-1 are independent from its PAP activity (Finck et al., 2006).

Phosphorylation is a mechanism used to regulate cellular localization of lipin-1 (Harris et al., 2007). Mammalian lipin-1 has been shown to become phosphorylated in response to insulin and amino acids and dephosphorylated in response to oleic acids and epinephrine (Huffman et al., 2002; Harris et al., 2007; and Kim et al. 2007). Expression of *Lpin1* is induced by presence of glucocorticoids, steroid hormones (Zhang et al., 2008).

The functional mechanisms of PAP have been studied for over 30 years, unlike the transcription activation mechanisms that remain mostly uncertain until today.

#### **D. Lipins in Mammals**

Lipin-1 gene was first described in 2001 (Péterfy et al., 2001). Since then, three *lipin* genes were identified in mammals, lipin-1, lipin-2, and lipin-3, which have been extensively studied in mice. It has been shown that lipin-1 deficiency in mice results in development of lipodystrophy and its overexpression results in obesity (Phan et al., 2005). Lipin-2 and lipin-3 were discovered after lipin-1 based on 60% amino acid identity (Péterfy et al., 2001). Each of the three *lipin* genes has a unique expression

pattern. Lipin-1 accounts for most of PAP activity in adipose tissue, bones, and muscles, but not in the liver (Donkor et al., 2007; Harris et al., 2007).

Correct expression of lipin-1 is essential for adipose differentiation and TAG storage (Péterfy et al., 2001; Phan et al., 2004). Transgenic studies in mice show that incorrect lipin-1 function in skeletal muscles leads to reduced fatty acid oxidation and thus obesity (Phan et al., 2005). Lipin-2 is mostly expressed in liver, kidneys, brain, and lungs; and lipin-3 has lower expression levels but is detectable in liver and visceral tissues (Donkor et al., 2007).

Various mutations in N-LIP domain of lipin-1 have been documented to be associated with metabolic disorders in humans (Péterfy et al., 2001). Lipin-1 deficiency was shown to cause muscle pain, weakness, and myoglobinuria in children (Zeharia et al., 2008). Unlike in mice, lipin-1 mutation does not cause lipodystrophy in humans, which may be explained by compensatory effects of lipin-2 (Donkor et al., 2007).

Silent mutations in C-LIP domain of lipin-1 have been shown to be associated with statin drugs treatment (Zeharia et al., 2008). These drugs are commonly used to treat hypercholesterolemia and some patients develop muscle pain and myopathy in response to the treatment (Sirvert et al., 2008).

Missense and nonsense mutations in C-LIP domain of lipin-2 have been shown to associate with recurring osteomyelitis, cutaneous inflammation, anemia, and psoriasis (El-Shanti et al., 2007; Ferguson et al., 2005; Majeed et al., 2001; and Milhavet et al., 2008).

Many studies have identified the importance of PAP and transcriptional coactivator function of lipin-1 in mice and humans. Specifically, a study by Nadra et al. shows that lipin-1 PAP deficiency in mice leads to fatty liver dystrophy (*fld*) mutant mouse strains (2008). This phenotype is described by accumulation of phosphatidate in adipose tissue and periphery leading to activation of mitogen-activated protein kinase/extracellular regulated kinase (MEK-Erk) in Schwann cells. The impact of the same mutation is not as severe in humans, but patients with lipin-1 deficiency also show significant accumulation of phosphatidate and its intermediates (Zeharia et al., 2008). An important feature of *fld* in mice worth mentioning is that these mutant animals develop fatty liver and hypertriglyceridemia during neonatal period (Langer et al., 1989). This finding indicates that PAP activity of lipin-1 is non-essential for hepatic TAG synthesis. Further studies suggest that PAP activity is not required for suppression of TAG synthesis; however, LXXIL, or transcriptional coactivator activity and PPAR $\alpha$  binding are required (Chen et al., 2008).

### **E. Use of *Drosophila melanogaster* in Studying Transcriptional Coactivator Functions of Lipin**

Unlike humans, *Drosophila melanogaster* possess only one *lipin* gene. Lack of the redundancy and high functional similarity between lipin-1 protein in mammals and *Drosophila* Lipin protein make the fruit fly a highly valuable asset in studying lipid metabolism.

*Drosophila* mechanism for lipid storage and processing is very similar to that in mammals. Lipids are stored in form of TAGs and cholesterol esters; both of these forms are primarily stored in the fat body of the animal, which is similar to the function of

mammalian adipocytes (Kuhnlein, 2011; Murphy, 2012). Along with oenocytes, dispersed clusters of cells located in the cuticle, fat body performs metabolic regulation of fat storage similar to mammalian liver (Gutierrez et al., 2007). In mammals,  $\beta$ -cells of the pancreas regulate carbohydrate and lipid metabolism (Saltiel and Khan, 2001). In *Drosophila*, the corpora cardiaca, a portion of the larval ring gland, secrete glucagon-like adipokinetic hormone (AKH) to fulfill the same function as pancreas in mammals (Kim and Rulifson, 2002). The genome of *Drosophila* contains seven genes that code for insulin-like peptides and the central brain contains insulin-producing cells, which have the same function as  $\beta$ -cells of the pancreas (Rulifson et al., 2002).

The goal of this study was to gain a better understanding of nuclear roles of lipin using *Drosophila melanogaster* as a model. It has been shown by Ugrankar et al. that *Drosophila* lipin is required for normal fat tissue development and normal animal development (2011). The nuclear localization signal (NLS) located in the NLIP region of the protein allows for lipin's translocation into the nucleus where it can then interact directly with transcription control proteins. The current project was divided into two major parts.

In the first part, CRISPR/Cas9 mutagenesis was utilized to generate a *lipin* allele lacking the NLS coding sequence. The expectation was to create a targeted double stranded break in the *lipin* gene and allow the DNA to be repaired used homology directed repair (HDR) mechanism using a template lacking the NLS coding sequence to generate a *Lipin $\Delta$ NLS*. The generated mutant was to be analyzed for significant phenotypic changes compared to controls.

The second part of the project focused on Lipin's nuclear functions in different tissues of *Drosophila*. Malpighian tubules and the ring gland were selected as the organs of interest based on previous observations of Lipin expression in the nucleus or the cytoplasm of these tissue (Ugrankar et al., 2011). It has been shown in the past that *Lipin $\Delta$ NLS* transgene has a dominant negative effect on the endogenous Lipin and prevents its translocation into the nucleus (Schmitt et al., 2015). The GAL4/UAS system was used to express Lipin $\Delta$ NLS or LipinWT (control) in the ring gland; in addition, Lipin[RNAi] expression was used in Malpighian tubules. In both cases, the data were collected as percent pupariation and the experimental groups were compared to the control groups using unpaired t-test.

The goal of the current study is to identify the nuclear function of Lipin and its effect on animal development. The hypothesis is that lipin's inability to translocate into the nucleus will cause developmental complication for the animals as well as prevent proper cell response to nutritional changes through defective gene regulation which would normally be controlled by Lipin as a transcriptional coactivator.

## **II. MATERIALS AND METHODS**

### **A. Fly Food Preparation**

Fly food was prepared in batches to make 6 L. The cauldron was first pre-heated at setting 8-9 (to allow water to boil). One hundred and eight grams of yeast were measured and combined with 600 mL of warm tap water and thoroughly mixed. Three hundred and sixty six grams of corn meal were added to yeast mixture and mixed thoroughly. In a separate container, 492 g of malt extract and 64 g of agar were combined. Once the cauldron reached the set temperature, 6 L of tap water were added.

Yeast and cornmeal mixture was immediately added to the water. Once the yeast and cornmeal have been mixed with water, agar and malt were slowly added while stirring. The food was brought to slow boiling and 78 mL of corn syrup were added. The food was allowed to cool to room temperature. Forty five mL of propionic acid and 60 mL of Tegosept were added and mixed. Once all ingredients were mixed, the food was distributed into vials with a sterile 60 mL syringe.

## B. Cloning of gRNA into pCFD3 Plasmid

Cloning of pCFD3 plasmid, Figure 1, (Addgene, Cambridge, MA, Cat.# 49410) was completed in order to introduce guide RNA (gRNA) to be used as a guide for Cas9 nuclease to the site for double stranded cut at NLS sequence of the *lipin* gene.

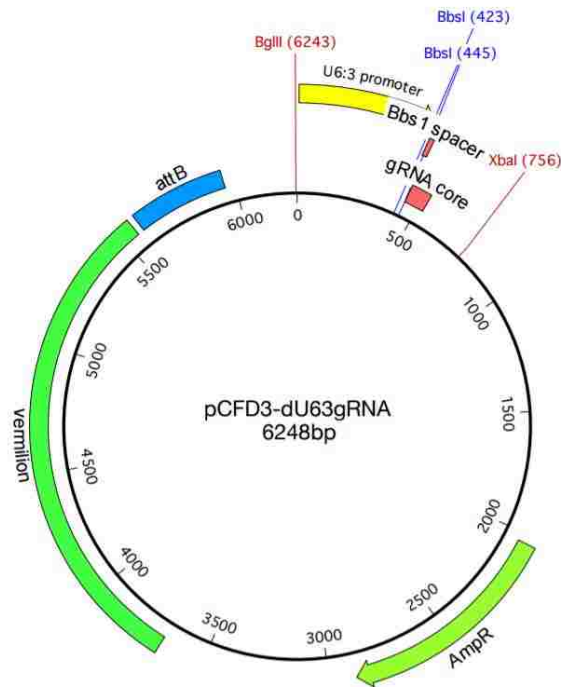


**Figure 1.** pCFD3 allows for expression of gRNA under control of the *Drosophila* U6:3 promoter. The plasmid has a pVallium22 backbone manufactured by Norbert Perrimon and Jian-Quan Ni at Harvard. pCFD3-dU6:3gRNA was a gift from Simon Bullock. Total vector size is 6,248 bp. The vector is ampicillin resistant. Ref: Optimized CRISPR/Cas tools for efficient germline and somatic genome engineering in *Drosophila* (Port et al., 2014).

The plasmid linearization was completed using Shrimp Alkaline Phosphatase (rSAP) protocol (New England Biolabs, Ipswich, MA, MO371). Plasmid, 6  $\mu\text{L}$ , 1  $\mu\text{L}$  Restriction Endonuclease (BbsI cut site), 5  $\mu\text{L}$  40x Restriction Enzyme Buffer, and 36  $\mu\text{L}$  of sterile water were combined and incubated at 37°C shaker overnight. The following day 2  $\mu\text{L}$  of rSAP were added to restriction digest (RED) and incubated for 1 hour at 37°C; at the expiration of the hour, rSAP was inactivated at 65°C for 20 minutes. The linearized plasmid was analyzed on a 0.7% agarose gel, which was ran for 30 minutes at 120 V to check for complete digestion. If the restriction digest was successful, all RED was ran on a 1% agarose gel for 30 minutes at 120 V. Following gel electrophoresis, the linearized plasmid was gel purified using QIAquick Gel Extraction Kit (Qiagen, Germantown, MD, 28704). The DNA was excised from the gel and weighed. The QG buffer was added to the DNA at the ratio of 3:1,  $\mu\text{L}$  to mg. The DNA and QG were incubated at 50°C for 10 minutes. The sample was vortexed and if a color change from yellow to orange was observed 10  $\mu\text{L}$  of 3 M sodium acetate were added. Isopropanol was then added to the mixture at ratio 1:1,  $\mu\text{L}$ , to the original weight of the gel in mg and the ingredients were thoroughly mixed. The mixture was then transferred to a column and span down at 13,000 rpm for 1 minute. The column was washed with 500  $\mu\text{L}$  of QG. Once the QG was discarded, the column was allowed to incubate at room temperature for 1 minute. The DNA was washed with 750  $\mu\text{L}$  of PE Buffer and the flowthrough was discarded. To elute DNA, the column was transferred to a sterile tube and 30  $\mu\text{L}$  of EB were added. The column with EB was incubated for 4 minutes after which the DNA was collected by centrifugation. The quality and quantity of the purified plasmid DNA were evaluated by running a 0.7% agarose gel for 30 minutes at 120 V. RED product was used as a control for size and quantity of circularized plasmid.

The oligonucleotides used for gRNA construction were different between the first CRISPR/Cas9 run and the next two, but in all cases the following general procedure was followed. The oligonucleotides were originally diluted in 1xTAE to concentration 100  $\mu\text{M}$ . PCR reaction was set up to anneal the ssOligonucleotides: 1  $\mu\text{L}$  of each ssOligonucleotide, 1  $\mu\text{L}$  T4 Ligation Buffer, 6.5  $\mu\text{L}$  sterile water, and 0.5  $\mu\text{L}$  T4 PNK (New England Biolabs). The thermocycler was set for hot start and the oligonucleotide annealing was completed at 37°C for 30 minutes, 95°C for 5 minutes, and cooled to 25°C at the rate of 5°C per minute. The quantity of oligonucleotide annealing was evaluated by gel electrophoresis. A 2% agarose gel was used to visualize annealed oligonucleotides. The gel was ran for 20 minutes at 120 V.

A ligation reaction for the oligonucleotides and the linearized plasmid was set up. Digested plasmid, 50 ng or 3.035  $\mu\text{L}$ , was combined with 1  $\mu\text{L}$  of annealed oligonucleotides at concentration of 1:200, 1.5  $\mu\text{L}$  10x T4 Ligation Buffer, 1  $\mu\text{L}$  of 1xT4 DNA Ligase, and 9.5  $\mu\text{L}$  of sterile water (New England Biolabs). Ligation took place at room temperature for 30 minutes. Circularized plasmid with gRNA was transformed into competent *E. coli*.

A laboratory stock of *E. coli* (DH5 $\alpha$ ) in glycerol kept at -80°C was thawed on ice for 20 minutes. Once the cells are thawed, 1:1 volume of 0.1 M sodium chloride was added. The purified ligation product, 10  $\mu\text{L}$ , was added to the cells and the ingredients were incubated on ice for 30 minutes. Following the incubation, the cells with ligation product were heat shocked at 42°C for 45 seconds and immediately transferred to ice for 2 minutes. To these cells, 800  $\mu\text{L}$  of optimal broth (SOB) with catabolite repression and added glucose (SOC) were added. The cells were then incubated at 37°C for 60 minutes while shaking at 225 rpm. Some of the incubated cells were then plated on Luria broth



(LB) agar plate with ampicillin (0.01 g ampicillin into 100 mL of liquid media), which was incubated at 37°C overnight. Leftover cells were centrifuged at 3,381 rcf for 2 minutes; the supernatant was then discarded until 200 µL were left, at which point cells were resuspended and plated on a second LB agar with ampicillin plate.

Five colonies of cells from the LB agar plate were transferred using aseptic techniques into 3 mL of LB plus ampicillin and incubated on shaker at 37°C overnight; these cells were used for the second and third round of CRISPR. Plasmid sequences were confirmed by sequencing with Eurofins (Louisville, KY) using primers:

5' sequencing primer ACCTACTCAGCCAAGAGGC

3' sequencing primer TGCATACGCATTAAGCGAAC

Once the plasmid sequencing results confirmed lack of secondary mutations and presence of gRNA, cells were preserved in glycerol as a stock at -80°C.

Clone 5 was obtained from -80°C and thawed. The culture was spread with a loop on LB-Amp plate and incubated at 37°C overnight. The following day, a colony from the LB-Amp plate was transferred into 3 mL of liquid LB-Amp (0.01 g ampicillin into 100 mL LB) and incubated at 37°C overnight while shaking. QIAprep Spin Mini Kit was used to harvest plasmid from the *E.coli* (Qiagen). The overnight culture of Clone 5 was centrifuged at 8,000 rpm for 3 minutes at room temperature. The cells were then resuspended in 400 µL Buffer P1 and transferred to microcentrifuge tubes. Four hundred µL of Buffer P2 were added to the tubes and the contents were mixed by inverting for no longer than 5 minutes. Next, 400 µL of Buffer N3 were added to the tubes mixed by inverting. The contents were centrifuged at 13,000 rpm for 10 minutes. The supernatant was extracted and applied to columns by pipetting. The columns were centrifuged at 13,000 rpm for 1 minute and the flowthrough was discarded. The columns were then

washed with 750  $\mu\text{L}$  of PE and centrifuged for 1 minute at 13,000 rpm. Following centrifugation, the flowthrough was discarded. The columns were then transferred to collection tubes and centrifuged at 13,000 rpm for 1 minute to ensure complete riddance of PE. After the expiration of 1 minute, the columns were again transferred to sterile collection tubes. The DNA was eluted with 30  $\mu\text{L}$  of EB. Once EB was added, the samples were incubated for 1 minute at room temperature and then centrifuged for one minute at 13,000 rpm. After centrifugation, the EB was transferred back into the columns, which were centrifuged as before one more time.

Plasmid concentration in the purified sample was determined by gel electrophoresis. A 0.7% agarose gel was made by adding agarose and 1 x TAE (Tris, glacial acetic acid, and 0.5 M EDTA). The mixture was first microwaved for 1 minute and mixed. After the initial minute, the solution was microwaved in intervals of 30 seconds until all agarose was dissolved. The solution was allowed to cool to room temperature at which point SYBR-Safe (Invitrogen, Thermo Fisher Scientific, Carlsbad, CA, #1821848) was added and the solution was slowly swirled. Once mixed, agarose was poured into a mold and allowed to polymerize for at least 30 minutes. Gel was loaded with 6  $\mu\text{L}$  of 1 kb ladder (New England Biolabs; lot# 1391612) in Sample Buffer at ratio 1:5 (New England Biolabs, lot#0141607) and 1  $\mu\text{L}$  of plasmid in 5  $\mu\text{L}$  of Sample Buffer. The electrophoresis was completed at 120 V for 30 minutes. The plasmid used for CRISPR injections had concentration 2-5  $\mu\text{g}/\mu\text{L}$ .

### **C. CRISPR/Cas9 Mutagenesis: Run I**

The use of CRISPR/Cas9 mutagenesis was intended to create a fly line that carries a *lipin* allele that lacks nuclear localization signal (NLS) in order to observe a loss of function (LOS) phenotype.

The preparatory steps for embryo injections included the following procedures. A gRNA CGACTTCTTGCGCCGCTTCT (TGG) (TGG is the PAM) was cloned into pCFD3 from Addgene using protocol from Eurofins as described above (Addgene, Cambridge, MA; Eurofins, Louisville, KY). A pair of oligonucleotides generated for cloning of the sgRNA into pCFD3 had the following sequences (Eurofins):

ProtoNLS 1: 5'-GTCGCGACTTCTTGCGCCGCTTCT-3'

ProtoNLS 2: 5'-AAACAGAAGCGGCGCAAGAAGTCG-3'

This cloning procedure generated gRNA, which was used as a guide for Cas-9 nuclease.

Single-stranded donor oligonucleotide (ssOligo) was synthesized complimentary to a portion of *lipin* at NLS but lacking NLS (Eurofins). This oligonucleotide was a donor used for homologous DNA repair with the following sequence:

5'-  
GACGTTAACCTCACCGGTCACAACCAGCGAAGCCACCAAGGAGGTGTCCAA  
GAGCAAAACCTCGCAAATGAAGAAGAATGCCAGCGCAAGAACTCTTCAAGCA  
GCTCATTGGGCAGCGCCGG-3'

Plasmid and the gRNA were combined by adding 50  $\mu$ L ultrapure water, pCFD3- $\Delta$ NLS at 500 ng/ $\mu$ L, and  $\Delta$ NLS ssOligo at 100 ng/ $\mu$ L. These components were then sent for embryonic injections into y[1] M{vas-Cas9}ZH-2A w[1118]/FM7c embryos (Bloomington Stock #51323; BestGene, Chino Hills, CA). Approximately 300 injected embryos were injected and sent to the laboratory.

Stable stocks were established for this CRISPR run using the general methodology described below in Section F (Establishing Stable Stocks); however, the

guide RNA that used here did not work properly so the section describes in detail only how CRISPR III stocks were established.

#### **D. CRISPR/Cas9 Mutagenesis: Run II**

Due to CRISPR I not being successful, a new gRNA was cloned into pCFD3 plasmid (Addgene). The new gRNA sequence was CCAAGAGCAAAACCAAGAAG (CGG) (CGG was the PAM).

The oligonucleotides (Eurofins) for cloning the gRNA were modified here:

ProtoNLS2-1: 5'-GTCGCCAAGAGCAAAACCAAGAAG -3'

ProtoNLS2-2: 5'-AAACCTTCTTGGTTTTGCTCTTGG-3'

The ssOligo used was the same as for CRISPR I (Eurofins). This oligonucleotide was a donor used for homologous DNA repair with the following sequence:

5'-  
GACGTTAACCTCACCACGGTCACAACCAGCGAAGCCACCAAGGAGGTGTCCAA  
GAGCAAAACCTCGCAAATGAAGAAGAATGCCCAGCGCAAGAAGCTCTTCAAGCA  
GCTCATTGGGCAGCGCCGG-3'

Plasmid and gRNA were co-injected into vas-Cas9 embryos (Bloomington #51323; BestGene, Chino Hills, CA) in a mixture combining 50  $\mu$ L ultrapure water, pCFD3- $\Delta$ NLS at 500 ng/ $\mu$ L, and  $\Delta$ NLS ssOligo at 100 ng/ $\mu$ L. Approximately 300 injected embryos were injected and sent to the laboratory.

The stable stocks were established for this CRISPR run using the general methodology described below in Section F (Establishing Stable Stocks); however, the

ssOligo donor that was used here did not work properly so the section describes in detail only how CRISPR III stocks were established.

### **E. CRISPR/Cas9 Mutagenesis: Run III**

The procedure for the third CRISPR run was identical to the previous times except a new 127-bp oligonucleotide designed according to rules defined by Richardson et al. (2016). The new information about CRISPR mutagenesis was different from what was known before. It was established that single-stranded oligonucleotide donor needs to be complementary to non-target strand (in other words that strain that contains PAM). The donor has to be asymmetric and overlap Cas9 cut site with 36 base pair PAM on distal side (upstream of PAM) and 91 base pair extension on PAM proximal side (downstream of PAM). In the first attempt at CRISPR the donor was generated correctly but the guide RNA did not work. In the second attempt at CRISPR, the donor was generated incorrectly but the guide RNA worked.

The single stranded oligonucleotide was generated at Integrated DNA Technologies (Coralville, IA). The sequence of the new oligonucleotide was as follows:

5'-  
GCGTCTCCGCCGAAGGCAAATCACCGCCGCCGGCGCTGCCCAATGAGCTGCTT  
GAAGAGTTCTTGCGCTGGGCATTCTTCTTCATTTGCGAGGTTTTGCTCTTGGAC  
ACCTCCTTGGTGGCTTCGCT -3'

The generated oligonucleotide was 39014.1 g/mole molecular weight and 4 nmole contained 156.06 µg.

## F. Establishing Stable Stocks

After the embryos were received from BestGene, the larvae were allowed to pupariate. The pupae were separated into individual vials to generate the founder (F) stock. A series of crosses was performed in order to establish balanced stocks for preservation of potential mutants.

The first cross was of the founder fly and a stock that carries a balancer marked with CyO on the second chromosome  $vas-Cas9/vas-Cas9$  (Y);  $Mut/+ \times w[*]$ ;  $P\{w[+mc]=GAL4-Hsp70.PB\}2/CyO, on1;2$ . Seventy six founder flies were crossed individually with four virgin females if they were males or with 3 males if they were female. Cy flies from the progeny (P) were selected for the next cross.

The second set of crosses was performed to introduce a balancer marked with CyO-GFP. The potential expected crosses were  $Vas-Cas9/+$  or  $Vas-Cas9/Y$  or  $+/Y$ ;  $Mut$  or  $+/CyO \times w$ ;  $P[w+; UASakt]1.1/CyO-GFP$ . Out of 76 original stocks 60 stocks were successful with the progeny to be used for the second set of crosses. For each of the 60 founder crosses, 3 flies were selected to be mated individually with flies carrying CyO-GFP to generate total of 120 crosses (F1). The procedure for these crosses was identical to the first set of crosses. GFP pupae were selected from each stock.

The adults that eclosed from selected pupae from the second cross (F1) were allowed to mate. The expected mating schemes were  $+/+(Y)$ ;  $Mut$  or  $+/CyO-GFP \times +/+(Y)$ ;  $Mut$  or  $+/CyO-GFP$  (this was our stock). Non-GFP pupae (F2) were selected from the progeny to establish homozygous stocks that potentially carry the mutation. If the cross produced only heterozygous progeny they were kept as a stock to be analyzed as well.

## **G. DNA Extraction from Single Flies**

Single flies from stocks of interest were transferred into individual tubes and kept on ice for 5 minutes. Squishing buffer was prepared on ice by mixing 965  $\mu\text{L}$  of distilled water, 10  $\mu\text{L}$  of 1M Tris-Cl, pH 7.4, 10  $\mu\text{L}$  100 mM EDTA, 5  $\mu\text{L}$  NaCl, and 10  $\mu\text{L}$  20 mg/mL proteinase K (New England Biolabs, #P8107S). Each fly was squished with a pipette tip and mixed with 50  $\mu\text{L}$  of Squishing Buffer. The samples were then incubated at room temperature for 20 minutes. Next, the samples were transferred to 95°C for 5 minutes. After heating, the samples were iced for 5 minutes and centrifuged for five minutes at 14,000 rpm. The DNA was stored at 4°C up to a week.

## **H. PCR Test for Mutations: CRISPR/Cas9 Run I**

Two different approaches were used to screen for Lipin $\Delta$ NLS mutants at this run. The first approach was to use two primer sets allowing us to evaluate presence of the mutation based on the product presence or size. The second approach was to use sequencing to evaluate the nucleotide composition of the flies in testing.

The goal of using the first set of primers was to have primers in which one of them would hybridize to the 18 nucleotides of NLS, meaning that if the NLS was excised using Cas9 then there would be no product visible on the gel and if the NLS was intact then the product size would be 201 base pairs. If the animals were to be heterozygous for  $\Delta$ NLS then the final product would appear less than in wild-type animals.

Primer pair 2 (NLS2F and NLS2R): 5' GGCGGACTCGGACTCGCTGGAC

3' TGCGACTTCTTGCGCCGCTTCTT

The second set of primers was used in order to visualize product size difference if the 18 base pair deletion took place. The primers were design to yield a very short

product. If the NLS was present then the product size would be 108 base pairs, and if the NLS was absent then the product size would be 90 base pairs.

Primer pair 4 (NLS4F and NLS4R): 5' AGCCACCAAGGAGGTGTCCAAGA  
3' GCGCTGCCCAATGAGCTGCTTGAA

The PCR reactions for the two sets of primers were set up similarly to each other with the exception of the primer type. The general master mix contained 12.5 µL of One Taq 2x Master Mix with GC Buffer (New England Biolabs, #04835), 2.5 µL One Taq High GC Enhancer (New England Biolabs, #B9026A), 2.5 µL 10 µM forward primer, 2.5 µL 10 µM reverse primer, 2.5 µL of sterile water and 2.5 µL of genomic DNA. The thermocycler setting included initial denaturation at 95°C for 3 minutes, following denaturation at the same temperature for 30 seconds, annealing at 64°C for PP2 or 62°C for PP4 for 30 seconds, extension at 72°C for 30 seconds, final extension at 72°C for 10 minutes and hold at 4°C. The number of cycles used was 30. Due to the small product size for primer pair 2 the gel electrophoresis was done on a 2% agarose gel; for primer pair 4, the gel electrophoresis had to be performed on a 3% agarose gel and using 50 bp ladder (New England Biolabs).

Sample sequencing was completed by Eurofins and two primer sets were used. The need for designing a separate primer set for sequencing purposes rose from the fact that the above product size were too small given the location of the NLS and the quality of sequencing reads. The first primer pair was (PP1):

5' CGCTGGACAACCAAAGCAAA  
3' CTTGGACAGGGGACTAGGGA

The second primer pair was (PP2):

5' CAAGGAGGAGCCCAAGGAAG



3' CTCCGTGTCGTCGAAGAAGT

The PCR reaction procedure for these two primer sets for sequencing was set up in the same way as described above. The thermocycler setting for the PP1 included initial denaturation at 95°C for 3 minutes, following denaturation at the same temperature for 30 seconds, annealing at 57°C for 30 seconds, extension at 72°C for 1 minute, final extension at 72°C for 10 minutes and hold at 4°C. The number of cycles used was 32. The thermocycler setting for PP2 were identical to those of PP1 for the exception of annealing temperature which was 59°C. The DNA was then processed as described in PCR purification, Gel electrophoresis, and Sending samples for sequencing sections.

### **I. PCR Test for Mutations: CRISPR/Cas9 Run II**

Oligo485's forward (5'-CGCTGGACAACCAAAGCAAA-3') and reverse (5'-CTCCGTGTCGCTGAAGAAGT-3') were used to amplify the template. The PCR reaction was set up for total volume of 50 µL by mixing 25 µL of 2x One Taq 2x Master Mix with GC Buffer, 5 µL of DNA template, 1 µL of forward primer 10 µM concentration, 1 µL reverse primer 10 µM concentration, and 18 µL of sterile nuclease-free water. The thermocycler setting were set up with initial denaturation for three minutes at 94°C, 94°C for 30 seconds as the first step of 30 cycles, annealing at 54°C for 30 seconds as the second step, extension at 68°C for one minute as the third step, final extension took place at 68°C for 10 minutes, and 4°C were held forever.

About half way through screening Oligo485 was likely contaminated and Oligo625's forward (5'-CAAACAGGCACACCGACAAC-3') and reverse (5'-TCCGTGTCGCTGAAGAAGTG-3') were used to amplify the template for second half of the samples. The PCR reaction was set up for total volume of 50 µL by mixing 25 µL of One Taq 2x Master Mix with GC Buffer, 5 µL of DNA template, 5 µL of forward primer 5

$\mu\text{M}$  concentration, 5  $\mu\text{L}$  reverse primer 5  $\mu\text{M}$  concentration, and 10  $\mu\text{L}$  of sterile nuclease-free water. The thermocycler setting were set up with initial denaturation for three minutes at 95°C, 95°C for 30 seconds as the first step of 30 cycles, annealing at 57°C for 30 seconds as the second step, extension at 72°C for one minute as the third step, final extension took place at 72°C for 4 minutes, and 4°C were held forever.

The DNA was processed as described in PCR purification, Gel electrophoresis, and Sending samples for sequencing sections.

### **J. PCR Test for Mutations: CRISPR/Cas9 Run III**

Oligo485's, same as used in CRISPR Run II analysis, were used to amplify the template. The PCR reaction was set up for total volume of 50  $\mu\text{L}$  by mixing 25  $\mu\text{L}$  of 2x One Taq Polymerase in Standard Buffer, 5  $\mu\text{L}$  of DNA template, 1  $\mu\text{L}$  of forward primer 10  $\mu\text{M}$  concentration, 1  $\mu\text{L}$  reverse primer 10  $\mu\text{M}$  concentration, and 18  $\mu\text{L}$  of sterile nuclease-free water. The thermocycler setting were set up with initial denaturation for three minutes at 94°C, 94°C for 30 seconds as the first step of 30 cycles, annealing at 54°C for 30 seconds as the second step, extension at 68°C for one minute as the third step, final extension took place at 68°C for 10 minutes, and 4°C were held forever.

The DNA was processed as described in PCR purification, Gel electrophoresis, and Sending samples for sequencing sections.

### **K. PCR Purification**

PCR products were column purified because the DNA was subsequently sequenced and Taq, other nucleotides, and primers used in the PCR reaction would interfere with sequencing reads if not removed. PCR product purification was accomplished using QIAquick PCR Purification Kit (Qiagen, 28106). A 5:1 volume of PB was added to empty tubes, which was used to precipitate DNA. PCR reaction was added

into PB. The contents of the tube were mixed thoroughly by inversion. If the mixture turned purple then 10  $\mu$ L of 3 M sodium acetate were added and mixed by inversion. The sample was then transferred to columns and centrifuged at 13,000 rpm for one minute. The flowthrough was discarded following centrifugation. Seven hundred and fifty  $\mu$ L of PE were added to the columns for DNA washing and the columns were centrifuged at 13,000 rpm for one minute. The flowthrough was discarded after centrifugation and the columns were centrifuged in the same manner as before the second time. The columns were transferred to sterile collection tubes after the second centrifugation. Lastly, 30  $\mu$ L of EB were used to elute DNA. EB was added to the center of the column and was incubated for one minute at room temperature. The samples were centrifuged for one minute at 13,000 rpm. Following centrifugation, the flowthrough was transferred back into the column and all samples were centrifuged at the same settings again.

#### **L. Testing Purified PCR Sample Concentrations by Gel Electrophoresis**

Before sending samples for sequencing, all purified PCR products were ran on either 0.7% or 1% agarose gel to test for purity and quantity to ensure successful sequencing results. The gels were freshly prepared by mixing 1xTAE with electrophoresis grade agarose (MP Biomedicals, Solon, Ohio, Cat #820723). The mixture was heated in a conventional microwave for one minute and stirred. The process was repeated at 10 second intervals until agarose was completely dissolved. The agarose in solution was then cooled to approximately 37°C and 10  $\mu$ L of SYBR-Safe DNA Gel Stain was added and mixed at that point (Thermo Fisher Scientific). The solution was then swirled and poured into prepared mold. The comb was inserted and the gel

was allowed to polymerize for at least 30 minutes. A 1 kb ladder (New England Biolabs, lot# 1391612) in Sample Buffer (New England Biolabs, lot# 0141607) in ratio 1:5 was used as a DNA size marker. Typically, 1  $\mu$ L of each sample in 5  $\mu$ L of Sample Buffer were run to test sample concentration. The gel was run at 100 V for 45 minutes.

### **M. Sending Samples for Sequencing**

All Sanger Sequencing was done by Eurofins. On average, 10  $\mu$ L of QIAquick purified PCR reactions at 42 ng/ $\mu$ L concentration were transferred into safe-lock tubes and shipped via one-day mail at room temperature.

### **N. Determining if Mutant Stocks Produced Homozygous Animals at Any Life Stages**

Once sequencing results were analyzed for presence of any mutations and non- $\Delta$ NLS mutants were identified a collection of all different mutants was generated. The mutants were analyzed for homozygosity and/or heterozygosity. The stocks were kept at 25°C for 24 hours and evaluated based on GFP expression at different life cycle stages. If the animals expressed GFP then they were considered heterozygous for mutation and if animals were non-GFP they were considered homozygous for mutation.

### **O. Analyzing Viability of Lipin Mutants and Determining Lethal Phase**

The stocks were also analyzed to determine their viability and lethal phase of mutation carrying homozygotes. To achieve this, heterozygous males (M/CyO-GFP) from the stocks that carry the mutation were crossed to virgins from Df(2R)Exel7095/CyO-GFP (Schmitt et al., 2015). The flies were allowed to lay eggs for 24 hours at 25°C. The pupae of this cross were evaluated based on GFP expression and the data was interpreted as percent of GFP over non-GFP pupa. When lethality was

observed, the crosses were further examined to determine the stage at which lethality took place (1<sup>st</sup>, 2<sup>nd</sup>, 3<sup>rd</sup> instar larva, or pupa).

### **P. Western Blot Analysis of CRISPR/Cas9 Mutants**

Some of non- $\Delta$ NLS mutant animals carried frame shift (FS) mutations leading to an early stop codon and truncating Lipin protein. Western blot was performed to visualize Lipin protein sizes that are present in FS mutants.

Whole protein was collected by dissecting all fat bodies from eight 3<sup>rd</sup> instar larvae in 1xPBST per 20 $\mu$ L of Sample Buffer (4 mL glycerol, 2 mL  $\beta$ -mercaptoethanol, 1 g SDS, 2.5 mL 1 M Tris-Cl pH 6.8, 0.5 mL sterile water, 0.8 mL 0.1% Bromophenol blue). Each sample was vigorously vortexed after every larva and all samples were heated at 95°C for 5 minutes. If the samples were not used immediately they were stored at -20°C. The samples were heated at 95°C for 5 minutes immediately before use.

Gel preparation was completed following protein extraction. Two glass plates for 0.75 mm gel were aligned together, small pieces of filter paper were placed between clamps of the plate holder and the plates and the clamps were closed. The glass plates were checked for alignment at the bottom. Petroleum jelly was used to seal the space at the bottom between two plates. The assembly was transferred to a plate rack and fixed with a clamp. Next, 15% (or 10%) resolving gel was prepared according the recipe by adding ingredients in the following order: 8x Lower Buffer, pH 8.8 (Tris 36.34 g, SDS 0.8 g, pH adjusted with HCl and water added up to 100 mL), 30% 0.8% bis-acrylamide (Acrylamide 60 g, bis-Acrylamide 1.6 g, 200 mL of water), 75% sucrose, pure distilled water, 5% ammonium persulfate, and TEMED. Resolving gel was transferred between two glass plates with a pipette until the solution reached the green bar of the plate holder. Isopropanol was pipetted over the resolving gel. The gel was allowed to dry at

room temperature for 30 minutes. After the expiration of 30 minutes, isopropanol was soaked out completely with filter paper. Stacking gel was prepared by mixing ingredients in the following order: 4x Upper Buffer, pH 6.8 (Tris 6.06 g, SDS 0.4 g, pH adjusted to 6.8 with HCl and water added to 100 mL), 30% 0.8% bis-acrylamide, pure distilled water, 5% ammonium persulfate, and TEMED was poured over the stacking gel and a 10 well 0.75 mm comb was inserted. The gel was allowed to dry for 30 minutes and used right away or stored covered by damp towel and wrapped with plastic wrap at 4°C for up to a week.

Electrophoresis of the gel was completed in 500 mL 1x Electrode Buffer (or Running Buffer). The gel, or two gels if applicable, were placed into a plastic frame with electrodes in such a way that the smaller glass plates face each other and locked into place then transferred to a plastic chamber. It was important to ensure that the inner chamber created by two plates was sealed well. The 1x Electrode buffer was poured into the inner chamber to the top of the plates and the rest of 500 mL was poured into the outer chamber. Six  $\mu\text{L}$  of Page Ruler Plus Prestained Protein Ladder were loaded as the size marker (Thermo Scientific, #26619, Waltham, MA). Ten  $\mu\text{L}$  (or as specified) of each sample were loaded following the ruler. The electrophoresis was conducted at P1 (200 V, 240 mA, 100 W) for 60 minutes.

Following electrophoresis, the gel was blotted onto a cellulose membrane (Immobilon P, Sigma-Aldrich, 0.45  $\mu\text{m}$  pore size). To prepare for blotting, two filter papers (Whatman, Sigma-Aldrich, 10427706x123429) per gel were cut to be the size of the gel (this step was optional if the filter paper fit the gel exactly). The cellulose membranes were pre-soaked in methanol for 5 minutes. The filter paper and the sponges were soaked in Transfer Buffer. The sandwich for transfer was assembled in the

following manner: cathode>transparent side of plastic cassette>one sponge>filter paper>membrane>gel>filter paper>one sponge>black side of plastic cassette>anode. The sandwich was fixed into position within plastic holder and then placed into a transfer chamber. Transfer Buffer was added to cover the entire sandwich. An ice block and a stirring bar were added to the chamber. Transfer was completed at P2 (100 V, 200 mA, 100 V) and ran for 90 minutes on a stirring plate.

All membranes were blocked in 5% BSA in 1xTBST for 2 hours at room temperature while shaking. Primary antibody staining was done using in house made anti-Lipin purified antibody generated to recognize NLIP domain of the Lipin protein (Ugrankar et al., 2011) diluted in 5% BSA in 1xTBST in concentration 1:1,000. The membranes were exposed to primary antibodies overnight, or 10 hours, at 4°C while shaking.

Prior to applying secondary antibody, the primary antibody was discarded and the membranes were washed 3 times for 5 minutes each in 1xTBST at room temperature while shaking. After washing, secondary antibody Alkaline Phosphatase-Conjugated Affinity Purified Goat Anti-Rabbit IgG (H+L) was applied (Jackson ImmunoResearch, #111989, West Grove, PA). Secondary antibody was diluted in 5% BSA in 1xTBST to concentration 1:1,000. Membranes were exposed to secondary antibody for 2 hours at room temperature while shaking.

At the expiration of 2 hours, secondary antibody was discarded and the membranes were washed with 1xTBST 3 times for 5 minutes at room temperature while shaking. Protein detection was completed with SigmaFast BCIP/NBT tablet (Sigma, St. Louis, MO, lot#SLBNo689V) diluted in pure water. The membranes were exposed for

10 minutes or until the bands were visible. Membrane development was stopped by using 10% acetic acid.

The membranes were allowed to dry and their images were taken. Membrane images were captured in BioRad Molecular Image Gel Doc, and software V5.0 (Irvine, CA). After opening the program, New Protocol option was selected. The following steps were conducted: Application>Blot>Colometric>Imaging Area; Gel Type>Bio-Rad Ready Gel; Color>Gray; Position Gel; No Filter; Run Protocol. All images were exported and saved in JPEG format.

### **Q. Whole Gene Sequencing of Lipin $\Delta$ NLS Mutant**

Once the NLS deletion was identified using Oligo485 it was important to ensure that no other secondary mutations occurred in the animals' genetic background, specifically in *lipin* gene. Whole gene sequencing was used to test for secondary mutations. SnapGene (GSL Biotech LLC Chicago, IL) was used to identify 11 primer pairs to cover the *lipin* gene including Lipin-RA cDNA (GH19076) start and 5' UTR through end sites with 3' UTR. Primer-BLAST (NCBI, Bethesda, MD) was used to design 22 primers. The following are sequences for 22 primers that were designed (Eurofins) (5' -> 3'):

Oligo771_PP1_NLS_F	AGCGGGAGAGAGAGATTGGA
Oligo771_PP1_NLS_R	AGAAAGGGGGCGAACAAACA
Oligo727_PP2_NLS_F	GATGGAGTCGGAGAGGGAGA
Oligo727_PP2_NLS_R	CTCCTGAGCACTCCCAGTTT
Oligo710_PP3_NLS_F	CCGCAGCAGACCAAAGATGA
Oligo710_PP3_NLS_R	ATGGTGTCGTTGGCCTTGTC
Oligo710_PP4_NLS_F	AGATGAAGCTGGGCGATTCT



Oligo710_PP4_NLS_R	TTGTGACCGTGGTGAGGTTA
Oligo720_PP5_NLS_F	GGACTCGCTGGACAACCAAA
Oligo720_PP5_NLS_R	GATTGGTGCTCGCTTTGCTG
Oligo705_PP6_NLS_F	GACGACCTTCGACTCCCATC
Oligo705_PP6_NLS_R	CGCAGTGAAGTGCTTGGAAC
Oligo745_PP7_NLS_F	CCATGTGCGGAATGTCGGAG
Oligo745_PP7_NLS_R	AGGTAGGCCGCGAAGTTTG
Oligo802_PP8_NLS_F	CGCCCAACCACTTGAACAAC
Oligo802_PP8_NLS_R	CTGCTCCGGCTTCTTCTCAA
Oligo738_PP9_NLS_F	CGAGCAAAACGGCTACAAGC
Oligo738_PP9_NLS_R	GATTGATTGAGTGGGGTGCG
Oligo778_PP10_NLS_F	GGTTCCGGTGTGCTCATT
Oligo778_PP10_NLS_R	ACTTAACTGGCCGACGAACT
Oligo705_PP11_NLS_F	GCGTCTCCACCAAAAACGAA
Oligo705_PP11_NLS_R	GCGCCAGTAGTTGAAGTTGG

The PCR reactions for each of the 11 primer pairs were set up on ice by combining 25  $\mu$ L of 2x One Taq in Standard Buffer (New England Biolabs, #M0482S), 5  $\mu$ L of template DNA, 1  $\mu$ L of 10  $\mu$ M forward primer, 1  $\mu$ L of 10  $\mu$ M reverse primer, and 18  $\mu$ L of sterile nuclease-free water.

NEB Tm calculator was used to determine Ta for each of the primers (Ipswich, MA). PP2, PP3, PP4, PP6, PP8, PP9, and PP10 were run at Ta of 56°C. PP1, PP5, and PP7 were run at Ta of 57°C. And PP11 was run at Ta of 55°C. The PCR cycle was set for initial denaturation at 94°C for three minutes, denaturation at 94°C as the first of 30

cycle steps, alternating Ta as the second step for 30 seconds, extension for one minute at 68°C as the third step, final extension for 10 minutes at 68°C, and hold at 4°C forever.

The PCR products were purified using QIAquick kit and the concentrations were established by running 1% electrophoresis gel at 100 V for 45 minutes. The samples were sent to Eurofins for sequencing.

Sequences were aligned to *lipin* genomic DNA in SnapGene and chromatogram peaks were confirmed using FinchTV V1.4 (Geospiza, American Fork, Utah).

### **R. Expression of Lipin $\Delta$ NLS or RNAi of Lipin in Malpighian Tubules**

UAS/GAL-4 system and/or RNAi were used to express *Lipin $\Delta$ NLS* transgene or downregulate Lipin in Malpighian tubules to study Lipin's nuclear localization function in the tissue on development of the animals.

There were two control crosses in the crossing scheme. The first control integrated a UAS-Lipin $\Delta$ NLS with  $w^{1118}$ , which should not have an effect because a wild-type animal does not carry a UAS responder.

UAS-Lipin $\Delta$ NLS x  $w^{1118}$  WBG

The second control cross combined a UAS responder, or driver, specific for tubule principal cells of Malpighian tubules (Bloomington #30835).

$w^{[*]}$ ; P{ $w[+mW.hs]=GawB$ }c42 x  $w^{1118}$  WBG

There were four experimental crosses. The first two crosses were intended to use two different drivers C42 and Uro-GAL4 (Bloomington #44416) for UAS-Lipin $\Delta$ NLS responder in order to overexpress Lipin $\Delta$ NLS in tubule principal cells of Malpighian tubules.

UAS-Lipin $\Delta$ NLS x  $w^{[*]}$ ; P{ $w[+mW.hs]=GawB$ }c42

UAS-Lipin $\Delta$ NLS x  $w^{[*]}$ ; P{Uro-GAL4.T}2

The second set of experimental crosses utilized UAS/GAL4 system and RNAi to block Lipin RNA decreasing protein production in the tubule principal cells of Malpighian tubules. The same drivers were used in these crosses as described above.

UAS-Lipin[RNAi]VDRC36007; on 2<sup>nd</sup> x w[\*]; P{w[+mW.hs]=GawB}c42

UAS-Lipin[RNAi]VDRC36007; on 2<sup>nd</sup> x w[\*]; P{Uro-GAL4.T}2

For all of the crosses, 10 virgins and 5 males were crosses per vial and the same batch of food was used for every vial. All animals were allowed to adopt and mate for 24 hours prior to beginning of the experiment. The first vial where animals were put together was not included in data analysis. All six crosses listed above were conducted in a biological triplicate, meaning that three independent vials with 10 virgins and 5 males were set up at the same time for each of six crosses. A drop of yeast paste was added to each vial to encourage mating. For the experiment, the flies were allowed to lay eggs for 6-8 hours during the day for three days at 29°C. The overnight vials were discarded. Once the pupae started forming, their count was taken for all vials every day at the same time of the day until no larvae were visible in the food.

All crosses were conducted in a biological triplicate and all crosses were replicated three times. Upon formation of the first pupae, the number of pupae was counted for all crosses every day until no pupae were coming up. The developmental data were analyzed as percent pupariation for each of the triplicates. The data were analyzed using unpaired t-test to compare the total pupariation percent per day for each of the crosses. The percent pupariation data was analyzed and the averages for pulled data from the biological replicates and normal replicates were plotted.

## **S. Immunostaining of Lipin in Malpighian Tubules and Fat Bodies**

Malpighian tubules and fat bodies from five *w<sup>1118</sup>* animals were dissected. Fat bodies were used as a positive control for Lipin antibody staining and were treated in the following steps together with Malpighian tubules. Both organs were fixed in 3.7% Formaldehyde in 1 x PBS (10 ml 37% formaldehyde and 90 mL 1 x PBS, pH 7.4) for 30 minutes at room temperature while shaking. The samples were then washed 4 times for 10 minutes with 1 x PBST while shaking at room temperature. The samples were blocked in 1 x PBST and Normal Donkey Serum (NDS) (Sigma-Aldrich) for 2 hours at room temperature while shaking. The primary anti-Lipin antibody (Ugrankar et al., 2011) was applied in concentration 1:200 diluted in 1 x PBST in NDS overnight at 4°C while shaking.

The following day, the primary antibody was discarded and the samples were washed 4 times for 10 minutes in 1 x PBST at room temperature while shaking. Secondary Cy3 Donkey anti-Rabbit antibody (Jackson ImmunoResearch Laboratories) diluted in 1 x PBST in NDS at 1:1,000 ratio was applied for 2 hours at room temperature while shaking. After the expiration of 2 hours, the samples were washed 4 times for 10 minutes in 1 x PBST. The samples were then transferred into a drop of SlowFading (Fisher Scientific) on a slide. A coverslip was applied over the sample and sealed with clear nail polish.

The images were captured using fluorescent microscope Axio Imager (Zeiss). Axiovision program was used to control microscope settings. The tissue was first located manually at total magnification of 25x. Once the desired focus was achieved, the magnification was adjusted to 100x and at this magnification the images were taken. Under the Multidimensional acquisition, Dye was selected as Cy3, Color – Orange,

Name – Cy3; During acquisition Workgroup was selected TRITC and After acquisition the FL closed was selected. Same settings were used for DAPI. In order to take pictures, the optimal exposure was measured first and all views were captured using the same exposure per one type of fluorescence. The exposure time for DAPI was 24 ms and for TRITC 1000 ms. Scale bars were added to the original images in the same program.

### **T. Expression of Lipin $\Delta$ NLS in the Ring Gland**

UAS/GAL4 system was utilized to express Lipin $\Delta$ NLS or LipinWT in different parts of the ring gland. Mai60 (Bloomington #30811) is a driver specific for prothoracic gland portion, where ecdysone is produced, and Aug21 (Bloomington #30137, CyO replaced by CyO-GFP in lab) is a driver specific for corpora allata portion, where juvenile hormone is produced.

The crossing scheme for this experiment included three controls. The first two crosses integrated either Lipin $\Delta$ NLS or LipinWT UAS responder into w<sup>1118</sup> background with no driver.

UAS-Lipin $\Delta$ NLS x w<sup>1118</sup> WBG

UAS-LipinWT x w<sup>1118</sup> WBG

The last control cross integrated a prothoracic driver Mai60, which may show a significant effect on animal development in experimental crosses due to the importance of proper ecdysone production to animal development, into a w<sup>1118</sup> background with no UAS responder. Aug21 was not expected to have a significant effect on the animal development and was thus not included in the control crosses.

P{GawB}Mai60 x w<sup>1118</sup> WBG

There were, in addition, three experimental crosses. The first two experimental crosses combined a UAS-Lipin $\Delta$ NLS responder with either Mai60 or Aug21 drivers.

Aug21 driver was prior crossed into a CyO-GFP background for internal control.

UAS-Lipin $\Delta$ NLS x P{GawB}Mai60

UAS-Lipin $\Delta$ NLS x w[\*]; P{w[+mW.hs]=GawB}Aug21/CyO-GFP

The last experimental cross combined a UAS-LipinWT responder with Mai60 driver.

UAS-LipinWT x P{GawB}Mai60

For all of the crosses, 10 virgins and 5 males were crosses per vial and the same batch of food was used for every vial. All animals were allowed to adopt and mate for 24 hours prior to beginning of the experiment. The first vial where animals were put together was not included in data analysis. All six crosses listed above were conducted in a biological triplicate, meaning that three independent vials with 10 virgins and 5 males were set up at the same time for each of six crosses. A drop of yeast paste was added to each vial to encourage mating. For the experiment, the flies were allowed to lay eggs for 6-8 hours during the day for three days at 29°C. The overnight vials were discarded. Once the pupae started forming, their count was taken for all vials every day at the same time of the day until no larvae were visible in the food.

All crosses were set up in biological triplicates and each one was repeated three times. Upon formation of the first pupae, the number of pupae was counted for all crosses every day until no pupae were coming up. The developmental data were analyzed as percent pupariation for each of the triplicates. The data were analyzed using unpaired t-test to compare the total pupariation percent per day for each of the crosses.

The percent pupariation data was analyzed and the averages for pulled data from the biological replicates and normal replicates were plotted.

### **III. RESULTS**

#### **A. Using CRISPR/Cas9 to Generate a Lipin $\Delta$ NLS Mutant**

Lipin is known to have two major functions in a cell: an enzymatic function, which allows conversion of phosphatidate phosphatase (PAP) to diacylglycerol (DAG) and transcriptional coactivator function (Vance et al., 2004). The goal of this project was to study the nuclear function of Lipin and the effects that would be caused by Lipin's inability to enter the nucleus. The primary question was: What will be the developmental effect on animals in which Lipin lacks the ability to enter cell nucleus? In other words, is nuclear localization of Lipin essential for proper animal development? The Lipin protein domain responsible for transcriptional co-activator activity is located in close proximity to PAP and the decision was made not to target this domain and instead focus on the protein sequence that allows nuclear translocation of Lipin. Nuclear localization signal (NLS) was chosen as a target for CRISPR/Cas9 to achieve sequence-specific *lipin* modification. The approach was to create a double stranded break in the *lipin* sequence within the NLS and use homology directed repair (HDR) mechanism for the DNA repair using a single stranded oligonucleotide that lacks NLS. As a result, the expectation was to generate a mutant that lacks 18 base pairs encoding the NLS. This deletion of NLS would be an in-frame mutation generating an otherwise normal Lipin protein, which is unable to enter the nucleus. CRISPR/Cas9 procedure was attempted three times in total. The majority of mutations that were generated, as a result, were caused by non-homologous end-joining (NHEJ). However, we were successful in identifying a Lipin $\Delta$ NLS mutant, which will be discussed in detail in the next section.

We also identified two in-frame mutations that caused a single amino acid deletion at position 276 and a triple amino acid deletion at position 273. The mutations that caused frame shift resulted in presence of a premature stop codon. As a result, all frame shift mutants were predicted to generate a truncated protein of about 300 amino acids on average; a normal Lipin protein has the length of 1089 amino acids. There were nine frame shift mutants total. Eight of those mutants resulted from nucleotide deletion at the site of Cas9 cut and one resulted from nucleotide insertion at the cut site. Figure 1 lists all mutant *lipin* alleles that were identified and specifies the sequence modifications as well as the effect on protein primary structure. The location of nucleotide modifications is described here in the relation to the location of the NLS. NLS starts at position 1304 of Lipin-RA cDNA.



Mutant Name	Location of the Nucleotide Modification with Respect to NLS	Nucleotide Modification	Protein Modification (Stop codon/amino acid Δ)
LipinΔNLS	0	ΔAAGAAGCGGCGCAAGA AG	ΔKKRRKK
LipinNLS_ IF276ΔK	0	ΔAAG	ΔK
LipinNLS_ IF273ΔKT K	-6	ΔAAAACCAAG	ΔTKK
LipinNLS0 Δ1FS284	0	ΔA	Stop 284
LipinNLS+ 2Δ1FS284	+2	ΔG	Stop 284
LipinNLS0 Δ2FS304	0	ΔAA	Stop 304
LipinNLS+ 2Δ5FS303	+2	ΔGAAGC	Stop 303
LipinNLS0 Δ5FS303	0	ΔAAGAA	Stop 303
LipinNLS- 3Δ7FS282	-3	ΔACCAAGA	Stop 282
LipinNLS- 6Δ13FS280	-6	ΔAAAAACAAGAAGC	Stop 280
LipinNLS- 47Δ47(+1)F S269	-47	ΔACGGTCACAACCAGCG AAGCCACCAAGGAGGTG TCCAAGAGCAAAAC,+G	Stop 269
LipinNLS+ 6(+2)FS28 5	+6	+AG	Stop 285

**Figure 2.** All CRISPR/Cas9 mutants generated and analyzed by sequencing. The top three lines of the table show in-frame mutants that were generated. One of these mutants was LipinΔNLS. The other nine mutants were caused by deletions or insertions of nucleotides that caused frame shifts. All mutants were analyzed for presence of a premature stop codon. The relative location of the mutations is presented in this table in relation to the start of the NLS sequence. The first nucleotide within NLS is annotated as 0; any nucleotide positions that comes before it has a negative number and any nucleotide position after it a positive number.

## B. Lipin $\Delta$ NLS Identification

The fly lines were tested for the deletion of NLS by sequencing. All fly lines that were tested were heterozygotes. The sequences were analyzed by manually aligning the nucleotides with double peaks to the wild-type sequence.

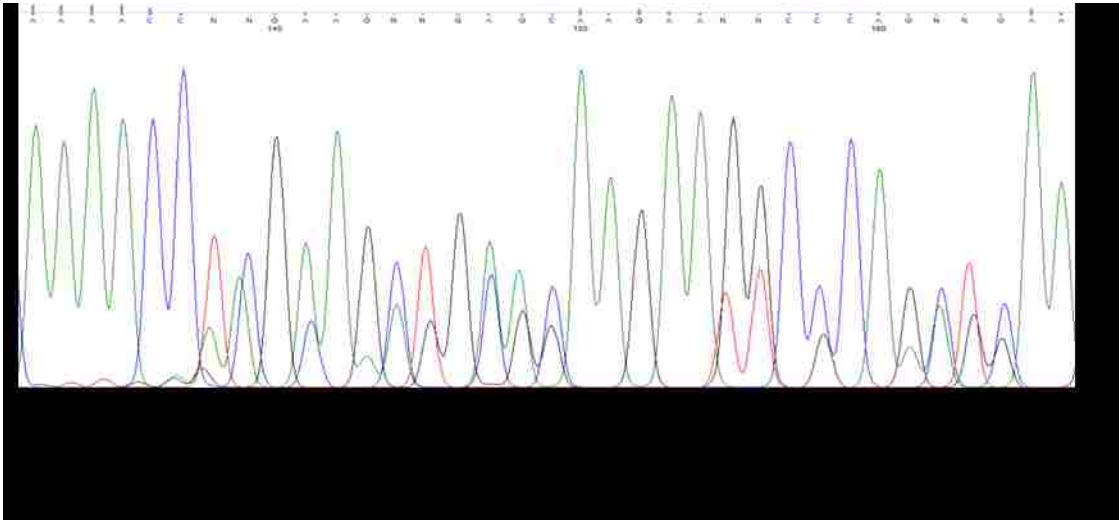


**Figure 3.** Partial sequence of genomic DNA from *lipin* locus of heterozygous Lipin $\Delta$ NLS larva. The *lipin* allele lacks the entire NLS coding region (AAGAAGCGGCGCAAGAAG encoding KKRRKK). The sequence located directly below the chromatogram is a portion of sequence of the wild-type *lipin* allele that matches a set of peaks in the chromatogram. The *lipin* locus lacking the NLS is located below the wild-type sequence and | indicates the point where the two sequences mismatch.

The sequence alignment indicates a wild-type sequence at the top and the modified sequence of the mutant *lipin* allele at the bottom. The bottom sequence lacks 18 nucleotides and thus generates double peaks as seen in the chromatogram in Figure 3.

The Lipin protein generated from the mutagenized sequence will lack the KKRRKK amino acids which NLS codes for. To conclude anything else about the mutant *lipin* allele, whole gene sequencing was done. The results of whole gene sequencing are discussed later.

Determination of *Lipin* $\Delta$ NLS allele presence was the initial step of the project. Once the mutant was identified, it was important to analyze the entire *Lipin* $\Delta$ NLS gene and protein for presence of secondary mutations before any further experiments may be conducted.

### **C. Testing *Lipin* $\Delta$ NLS Mutant for Presence of Secondary Mutations**

The *Lipin* $\Delta$ NLS mutant allele generated by CRISPR/Cas9 mutagenesis was analyzed for secondary mutations by sequencing. This measure was taken to ensure that any phenotype observed is only due to the loss of NLS. Eleven primer pairs were generated that span the region of the *lipin* gene encoding Lipin-RA transcript covering sequence starting at the second downstream promoter. The data generated by sequencing was compared to the genomic DNA of the wild-type by aligning the sequences in SnapGene (GSL Biotech LLC). *Lipin* genomic DNA was retrieved from FlyBase and nucleotide numbering used in Figure 4 was determined by assigning transcription start site "+1." The regions covered by sequencing were the following: transcription start site, 5'UTR, all 11 exons, stop codon, 3' UTR, and all but first two introns. The sequences were analyzed for any mutations in SnapGene. Twenty six mutations were found. Eight single nucleotide exchanges take place in upstream sequence in relation to the promoter. There is also one single nucleotide exchange in 5' UTR. Six of these mutations were single nucleotide exchanges in the intron regions of the *Lipin* $\Delta$ NLS allele. One single nucleotide exchange on mutant allele caused an amino acid change from phenylalanine to tyrosine in position 39. Two single nucleotide exchanges present on the mutant allele only caused no amino acid change in the protein sequence. Another two single nucleotide exchanges were a result of naturally occurring

polymorphism and they were the same for both *lipin* alleles. The first polymorphism resulted in amino acid change from threonine to serine and the second caused a change from asparagine to aspartate. The mutant allele also contains three single nucleotide exchanges in the 3' UTR; and both alleles contain a two nucleotide insertion (AA) in 3' UTR. Lastly, the mutant allele contains a single nucleotide exchange in the downstream sequence.

Nucleotide Position	Nucleotide Change	Amino Acid Position	Amino Acid Change	One/Both Alleles are Affected	Region Affected
-299	T->A	-	-	one	UP
-239	A->C	-	-	one	UP
-236	A->C	-	-	one	UP
-208	G->T	-	-	one	UP
-186	T->C	-	-	one	UP
-169	C->G	-	-	one	UP
-108	T->C	-	-	one	UP
-21	C->T	-	-	one	UP
+25	C->T	-	-	one	5' UTR
+298	G->A	-	-	one	intron
+3272	T->A	39	F->Y	one	exon
+3368	T->C	-	-	one	intron
+3446	C->A	-	-	one	intron
+3449	A->T	-	-	one	intron
+4460	ΔAAGAAG CGGCGCA AGAAG	275	ΔKKRR KK	one	exon
+5269	C->T	544	-	one	exon
+5522	C->G	-	-	one	intron
+5553	T->C	-	-	one	intron
+5922	T->C	663	-	one	exon
+6209	C->G	718	T->S	both	exon
+7616	A->G	1047	N->D	both	exon
+7735	G->C	-	-	one	3' UTR
+7714	T->G	-	-	one	3' UTR
+7715	A->G	-	-	one	3' UTR
+7801	+AA	-	-	both	3' UTR
+8010	T->A	-	-	one	DN

**Figure 4.** *Lipin*ΔNLS allele sequencing results. Heterozygous animals carrying *Lipin*ΔNLS were sequenced and both alleles were compared to each other and to the genomic sequence available on Flybase to test for secondary mutations and/or naturally occurring polymorphisms. UP-upstream; DN-downstream.

#### **D. Genetic Complementation between Lipin $\Delta$ NLS and Lipin $\Delta$ PAP**

*Lipin $\Delta$ NLS* as well as *Lipin $\Delta$ PAP* are recessive lethal alleles. These alleles are maintained over a balancer chromosome that carries a CyO-GFP marker. Expression of GFP by the balancer chromosome allows for easy identification of animals homozygous or heterozygous for the mutation. The balancer chromosome carries a recessive lethal allele, which means GFP marks only heterozygous individuals. We performed a cross between *Lipin $\Delta$ NLS* and *Lipin $\Delta$ PAP* flies to determine whether the two alleles can complement one another and *Lipin $\Delta$ NLS/Lipin $\Delta$ PAP* animals are viable. Another cross performed was between *Lipin $\Delta$ PAP* and *w<sup>1118</sup>*. The potential expected genotypes from the crosses are following.

For cross 1 *Lipin $\Delta$ NLS/CyO-GFP* x *Lipin $\Delta$ PAP/CyO-GFP*:

*Lipin $\Delta$ NLS* / *Lipin $\Delta$ PAP*

*Lipin $\Delta$ NLS* / *CyO-GFP*

*Lipin $\Delta$ PAP* / *CyO-GFP*

About 30% percent of all offspring are expected to be transheterozygous for the mutant *lipin* alleles if they are viable. These offspring will be non-GFP. The other about 70% of the offspring are expected to be GFP and heterozygous for one of the mutant *lipin* alleles.

For cross 2 *Lipin $\Delta$ PAP* / *CyO-GFP* x *w<sup>1118</sup>* we expect 50% of the offspring to be heterozygous for the *Lipin $\Delta$ PAP* allele (non-GFP) and 50% to carry two wild-type *lipin* alleles (GFP).

Figure 5 shows the distribution of the offspring of crosses described above. The ratio of non-GFP to GFP pupa indicates that animals who carry *Lipin* $\Delta$ NLS / *Lipin* $\Delta$ PAP are viable. No obvious developmental delays and pupae size differences were observed. The animals were observed into adulthood and both, non-GFP labeled and GFP labeled animals produced adults.

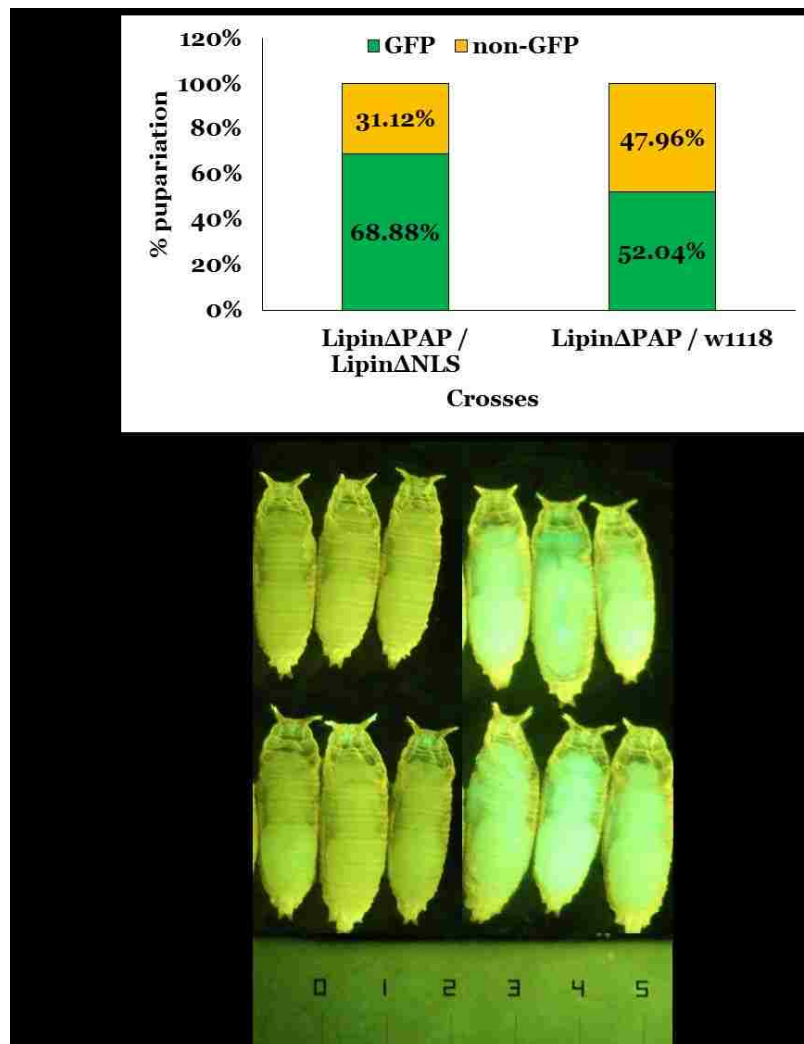


**Figure 5.** Animals that are transheterozygous for *Lipin* $\Delta$ NLS and *Lipin* $\Delta$ PAP are viable. GFP is used as a marker for wild-type balancer chromosome and the animals that do not display GFP carry only mutant alleles of *lipin*, *Lipin* $\Delta$ NLS and *Lipin* $\Delta$ PAP. (A) The ratio of non-GFP to GFP pupae that were counted for each cross were as expected, if animals transheterozygous for *Lipin* $\Delta$ NLS and *Lipin* $\Delta$ PAP are fully viable. (B) Pupae formed by *Lipin* $\Delta$ NLS/*Lipin* $\Delta$ PAP larvae are of normal size (non-GFP left half, GFP right half; tick marks on the ruler are 1 mm.)

## E. Characterization of Non- $\Delta$ NLS Mutant *Lipin* Alleles Created by CRISPR/Cas9 Mutagenesis

Most of non- $\Delta$ NLS mutant *lipin* alleles exhibited homozygous lethality. All mutants were analyzed for homozygous lethal phase (Figure 6).

Mutant Names	Embryo	1 <sup>st</sup> Instar Larva	2 <sup>nd</sup> Instar Larva	3 <sup>rd</sup> Instar Larva	Pre-pupa	Pupa	Adult
<b>Lipin<math>\Delta</math>NLS</b>	+	-	-	-	-	-	-
<b>LipinNLS_IF276<math>\Delta</math>K</b>	+	+	+	+	+	+	+
<b>LipinNLS_IF273<math>\Delta</math>KTK</b>	+	+	-	-	-	-	-
<b>LipinNLS<math>\Delta</math>1FS284</b>	+	-	-	-	-	-	-
<b>LipinNLS+2<math>\Delta</math>1FS284</b>	+	-	-	-	-	-	-
<b>LipinNLS<math>\Delta</math>2FS304</b>	+	-	-	-	-	-	-
<b>LipinNLS+2<math>\Delta</math>5FS303</b>	+	-	-	-	-	-	-
<b>LipinNLS<math>\Delta</math>5FS303</b>	+	-	-	-	-	-	-
<b>LipinNLS-3<math>\Delta</math>7FS282</b>	+	-	-	-	-	-	-
<b>LipinNLS-6<math>\Delta</math>13FS280</b>	+	+	-	-	-	-	-
<b>LipinNLS-47<math>\Delta</math>47(+1)FS269</b>	+	-	-	-	-	-	-

**Figure 6.** Lethal phase analysis of *lipin* mutants generated in this study. The “+” sign indicates presence of live homozygous animals for the *lipin* allele at the developmental stage listed. The “-” sign indicates presence of only heterozygous animals at the developmental stage specified.

It was observed that only one in-frame mutant lacking a lysine of the NLS made it to adulthood as a homozygote (IF\_276 $\Delta$ K). The other in-frame mutant (beside *Lipin $\Delta$ NLS*) had a lysine-threonine- lysine deletion causing early lethality at 1<sup>st</sup> instar larval stage (IF\_273 $\Delta$ KTK). Two of eight frame shift mutants were observed as 1<sup>st</sup> instar larvae but not past this stage. The rest of the frame shift mutants and *Lipin $\Delta$ NLS* animals did not generate any homozygotes at any stage past embryo.

## F. Analysis of CRISPR/Cas9 Mutagenized Animals for Secondary Mutations

The data we obtained for the lethality stage of CRISPR/Cas9 mutant animals show that animals carrying two copies of the mutant allele exhibit early lethality. This



applies to all alleles except Lipin IF\_276ΔK. To exclude that CRISPR/Cas9 mutagenesis caused secondary unintended mutations that caused the lethal phenotype, we analyzed lethality of animals that carried the mutagenized chromosome over a different chromosome that carried a deletion of the *lipin* locus (Df(2R)Exel7095). The scheme for all conducted crosses is Mut /CyO-GFP x Df(2R)Exel7095/CyO-GFP. This cross results in offspring of the following genotypes:

Mut / Df(2R)Exel7095

Mut / CyO-GFP

Df(2R)Exel7095 /CyO-GFP

From these expected outcomes we can determine whether Mut / Df(2R)Exel7095 genotype is viable by analyzing presence of GFP in the offspring. Presence of non-GFP animals signifies that Df(2R)Exel7095 chromosome that does not contain a functional copy of Lipin was able to rescue the animal carrying a mutant *lipin* allele. If that was the case, then we would know that there is a secondary mutation present on the mutagenized chromosome and that the mutant *lipin* allele is in fact functional and can rescue the deficiency chromosome.

Our data indicate that selected frame shift mutants used for this cross showed no rescue by the deficiency chromosome (Figure 7). This means that these animals indeed do not contain a functional copy of *lipin* and that lethality is not caused by a second-site mutation. Previously, we observed early larval lethality of homozygous flies with a *lipin* allele causing KTK deletion in the NLS region. However, a cross of these animals with Lipin deficiency animals resulted in no lethality. This outcome indicates that the

observed lethality was indeed caused by a second site mutation and not by the KTK deletion. Before these animals may be used for further experiments, the second-site mutation needs to be removed from the chromosome by genetic recombination.

Mutant Name	Success of Complementarity
LipinNLS $\Delta$ 2FS304	Lethal
LipinNLS-3 $\Delta$ 7FS282	Lethal
LipinNLS+6(+2)FS285	Lethal
LipinNLS_IF273 $\Delta$ KTK	Non lethal
LipinNLS_IF276 $\Delta$ K	Non lethal

**Figure 7.** Frame shift mutants derived from CRISPR/Cas9 lines were crossed with Df(2R)Exel7095/CyO-GFP. Flies carrying a copy of *lipin* with a frameshift mutation were not able to survive. The animals carrying an in-frame *lipin* mutation were able to survive over the deficiency allele.

### G. Testing Mutant Animals for Predicted Lipin Protein Product Sizes

It was mentioned earlier that *lipin* alleles that contain-frame shift mutations are expected to produce Lipin protein of reduced size. The in-frame deletion mutation also will cause a change in the final Lipin protein size but it will be insignificant (1 or 3 amino acids from 1089). Western blot protocol was used in order to visualize and analyze if the predicted protein sizes for the mutants can be observed. In order to achieve this goal, whole fat bodies from 3<sup>rd</sup> instar larvae were dissected and the total protein was extracted. The *w<sup>1118</sup>* animals were used as a control. The protein of the samples was run on an SDS-PAGE gel. A polyclonal anti-NLIP domain of Lipin primary antibody was used (even the truncated proteins should be detected). The first gels were produced using 15% resolving gel and loading 10  $\mu$ L of each sample. Figure 7 shows the images of the gels obtained from this set up.

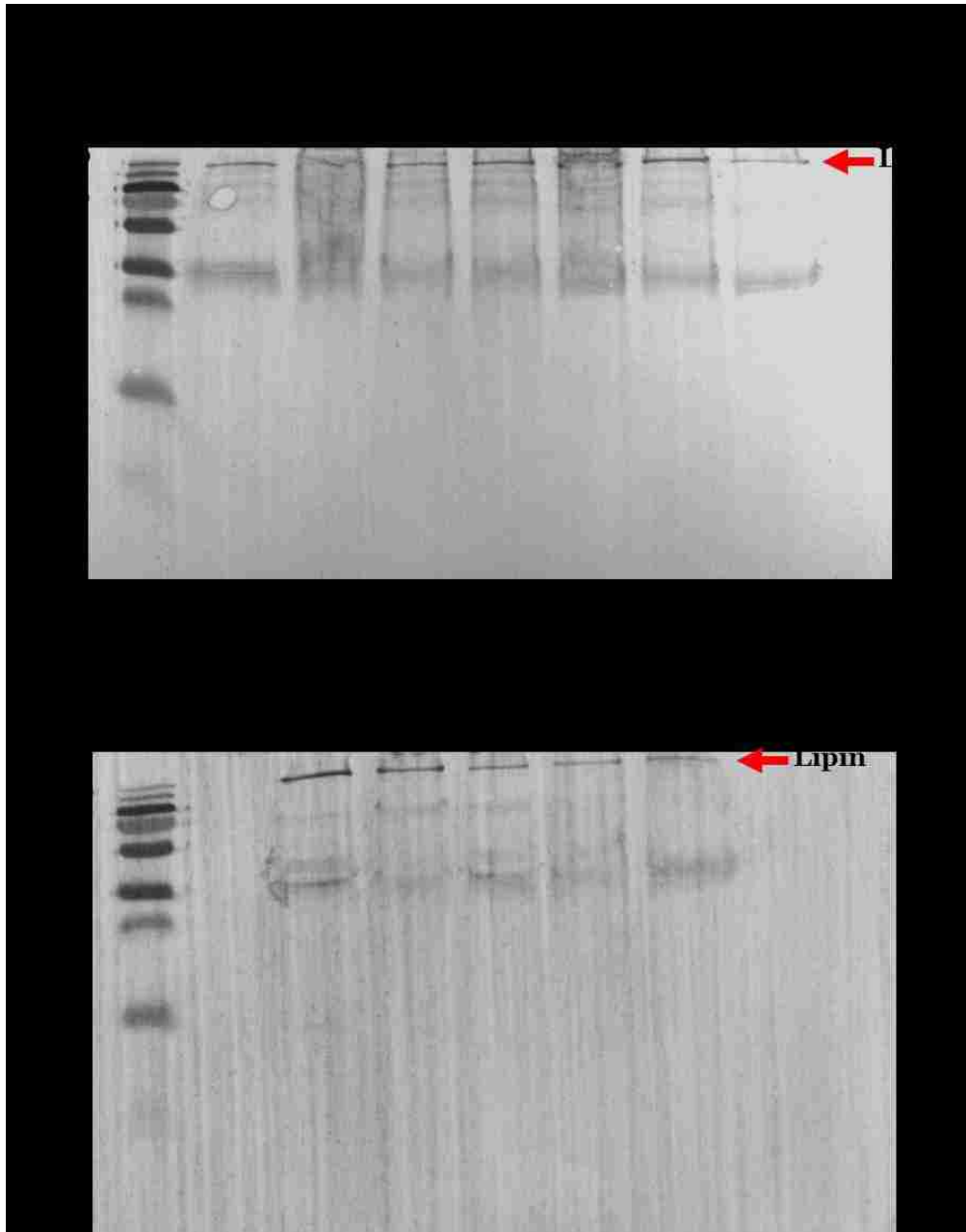


**Figure 8.** Heterozygous *lipin* mutants that carry frameshift mutations express a full-length Lipin protein but the expected truncated protein is not observed (15% resolving gel). (A) Loading sequence: 1-Protein ruler, 2- $w^{1118}$ , 3-LipinNLS $\Delta$ 2FS304, 4-LipinNLS+2 $\Delta$ 1FS284, 5-LipinNLS+2 $\Delta$ 1FS284, 6-LipinNLS+2 $\Delta$ 5FS303, 7-LipinNLS-6 $\Delta$ 13FS280, and 8-LipinNLS-3 $\Delta$ 7FS282. (B) Loading sequence: 1-Protein ruler, 2-empty, 3-Lipin $\Delta$ NLS, 4-LipinNLS+6(+2)FS285, 5-LipinNLS-47 $\Delta$ 47(+1)FS269, 6-LipinNLS $\Delta$ 1FS284, and 7- $w^{1118}$ .

The expected protein size for wild-type Lipin is approximately 220 kDa. The expected size for the truncated proteins as a result of an early stop codon in-frame shift mutants ranges from 29 kDa to 33 kDa. Unfortunately, all protein samples that were run show a diffuse band in the region where the truncated protein would be expected to be, including the control. These outcomes are likely due to protein degradation that has taken place. It is possible that the truncated protein is present but it can either be covered by the degradation product of the same size or the truncated protein simply cannot be visualized at the used total protein concentration. The truncated protein may not be visualized if the amount of antibody that binds to it is too low. In that case we would see nice bands for wild-type Lipin and the truncated Lipin that is also produced may be just below the detection levels.

To test the first scenario of low detection threshold, the samples were re-run at twice the concentration as before. A 10% resolving gel was used this time to allow for better separation of the bands that can potentially be very close in size. Figure 8 shows the outcomes of the second run. There was an increase of degradation products that made proper evaluation of the results impossible.

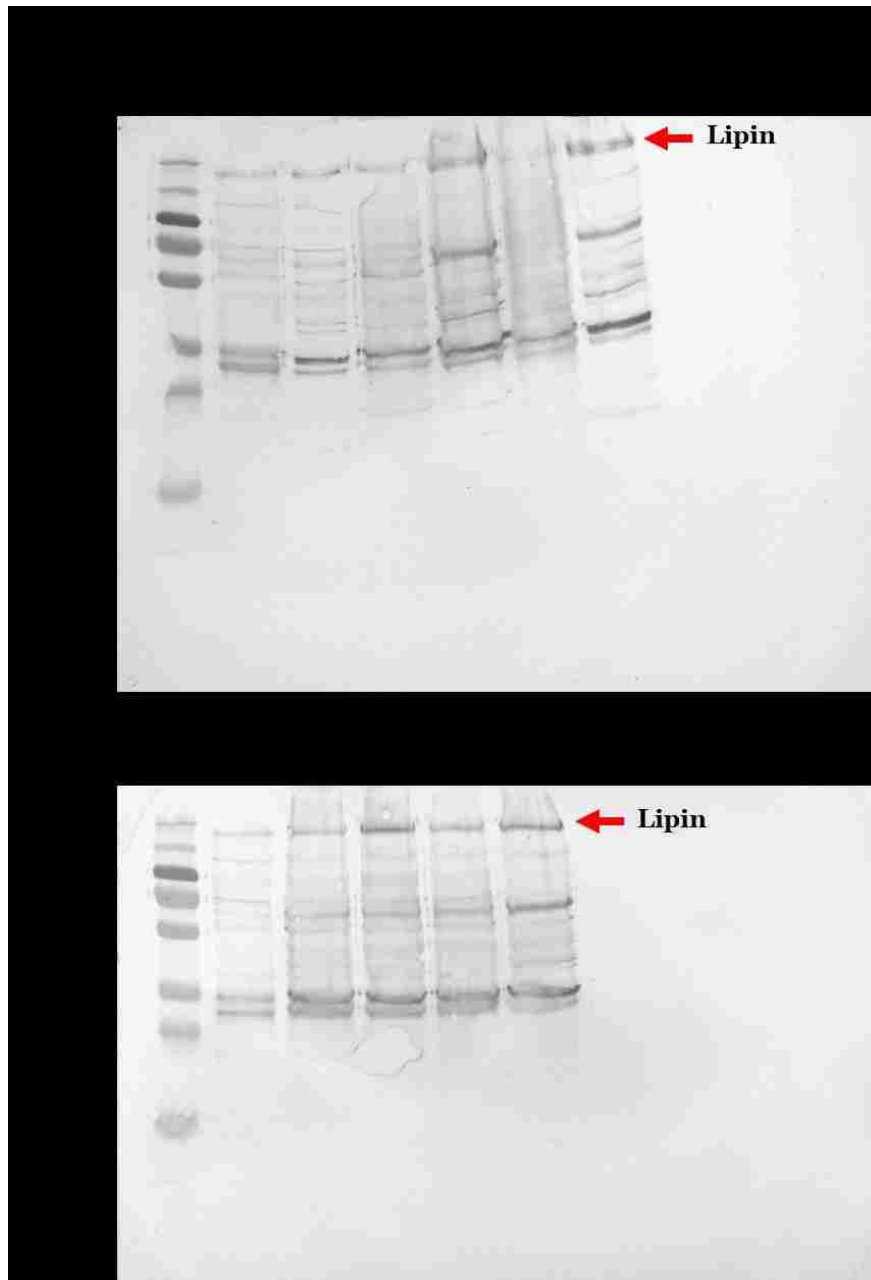


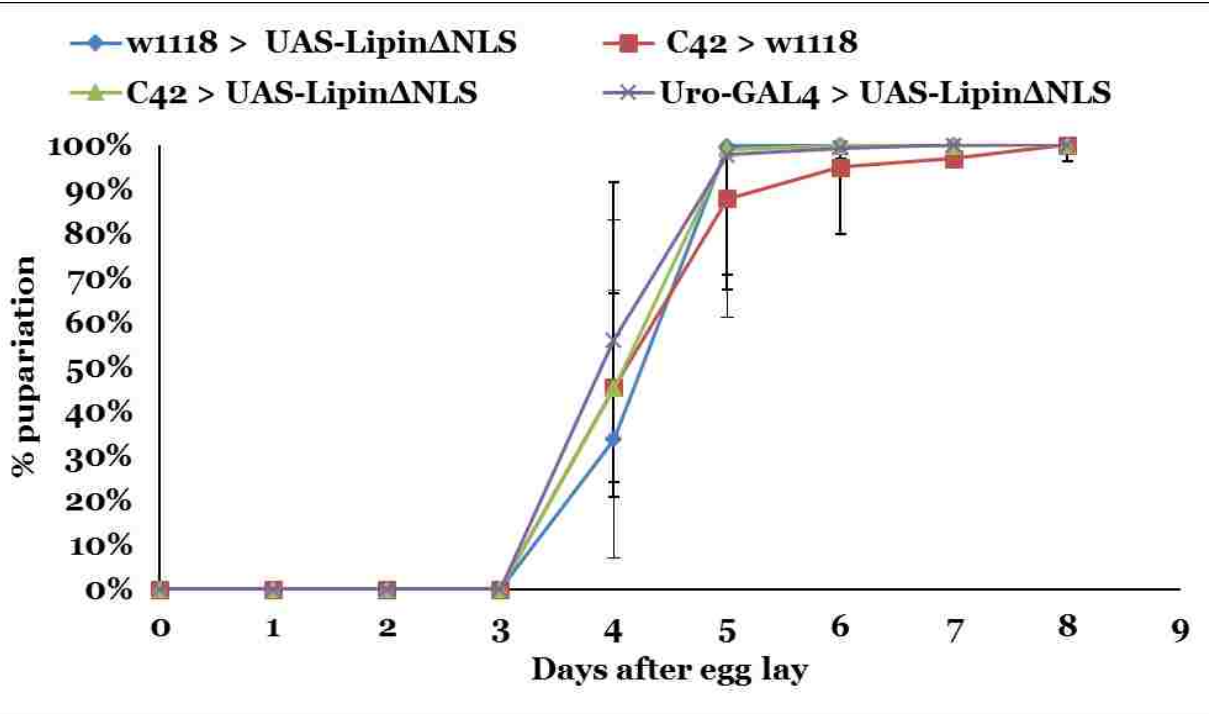
**Figure 9.** Heterozygous *lipin* mutants that carry frameshift mutations in a single copy of *lipin* gene express a full length Lipin protein but the expected truncated protein is not observed (10% resolving gel). (A) Loading sequence: 1-Protein ruler, 2- $w^{1118}$ , 3-LipinNLS $\Delta$ 1FS284, 4-LipinNLS+2 $\Delta$ 1FS284, 5-LipinNLS-47 $\Delta$ 47(+1)FS269, 6-LipinNLS $\Delta$ 2FS304, and 7-Lipin $\Delta$ NLS. (B) Loading sequence: 1-Protein ruler, 2- $w^{1118}$ , 3-LipinNLS-3 $\Delta$ 7FS282, 4-LipinNLS+2 $\Delta$ 5FS303, 5-LipinNLS-6 $\Delta$ 13FS280, and 6-LipinNLS+6(+2)FS285.

## H. Function of Lipin in Malpighian Tubules

The importance of nuclear functions of Lipin in different tissues of *Drosophila* is not understood. Malpighian tubules in the larvae of *Drosophila* are excretory organs similar to the kidneys of vertebrates. It has been shown that  $w^{1118}$  animals exhibit strong nuclear localization of Lipin in their Malpighian tubules under standard conditions (Ugrankar et al., 2011). It has also been shown that Lipin $\Delta$ NLS has a dominant negative effect on endogenous Lipin and prevents it from nuclear entry (Schmitt et al., 2015). The function of Lipin in the nucleus of Malpighian tubules is not understood and thus this part of the project focused on answering if exclusion of Lipin from the nucleus leads to a detectable phenotype. If Lipin $\Delta$ NLS is expressed in tubule principal cells of Malpighian tubules, will the development of larvae be affected? If the level of Lipin is downregulated via RNAi, will there be an effect on development of the larvae?

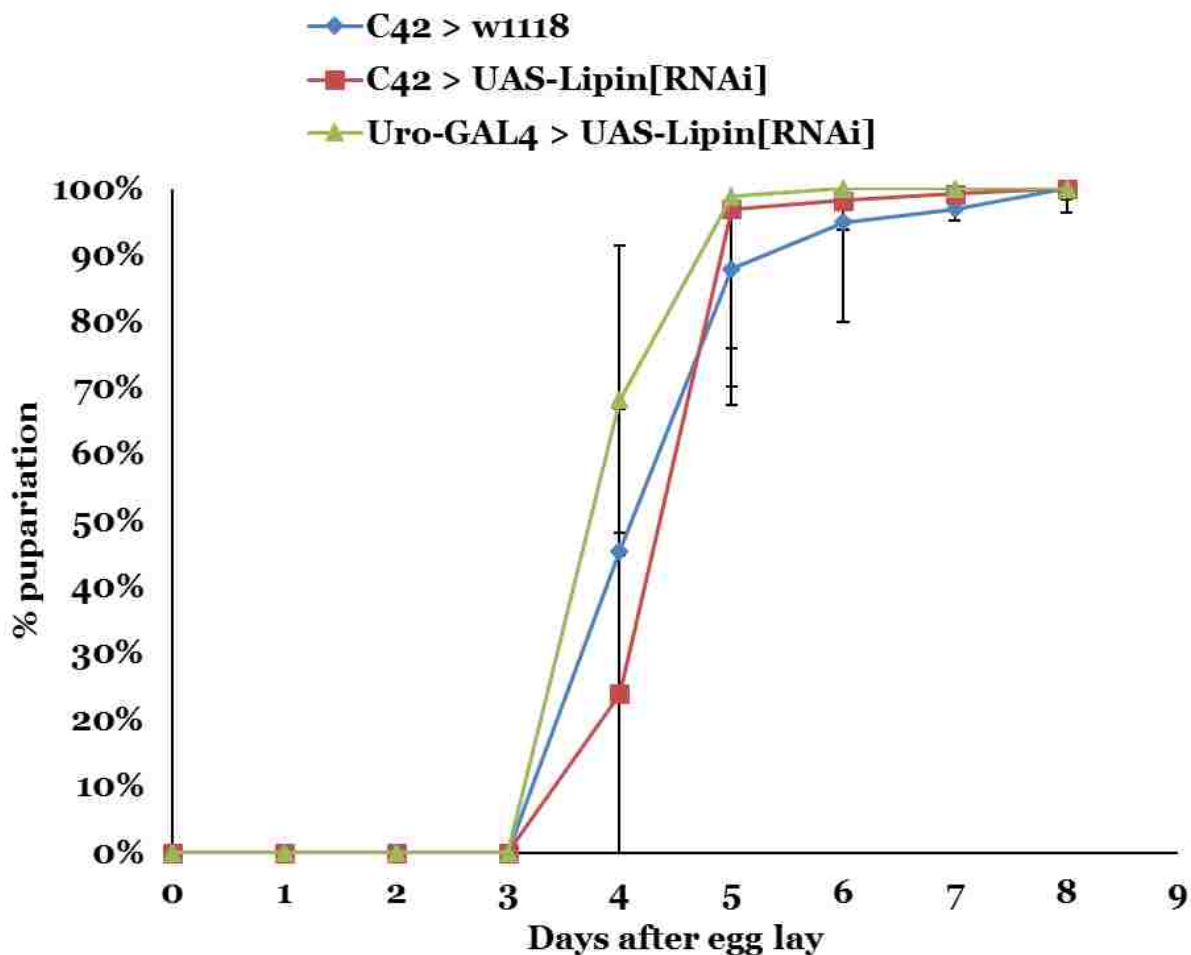
To answer these questions, the UAS/GAL4 system was used in order to target Malpighian tubules only and either express Lipin $\Delta$ NLS or Lipin[RNAi]. Two drivers for Malpighian tubules were used for both experiments, C42 and Uro-GAL4. UAS-Lipin $\Delta$ NLS, UAS-Lipin[RNAi], and UAS-LipinWT were the responders used in this experiment. UAS-LipinWT was used as a control.

Figure 9 shows the outcomes of expressing Lipin $\Delta$ NLS in Malpighian tubules using C42 and Uro-GAL4. The crosses between  $w^{1118}$  and either UAS-Lipin $\Delta$ NLS or C42 were used as controls. Comparing the two experimental groups, C42 > UAS-Lipin $\Delta$ NLS and Uro-GAL4 > UAS-Lipin $\Delta$ NLS, to the control groups, no statistical difference was determined (unpaired t test;  $p > 0.05$ ).



**Figure 10.** Overexpression of LipinΔNLS in Malpighian tubules using C42 or Uro-GAL4 drivers. When LipinΔNLS is overexpressed using C42 or Uro-GAL4 there is no developmental effect on the animals ( $p > 0.05$ ).

The same strategy was used for analyzing the outcomes of RNAi experiment. This time C42 /  $w^{1118}$  was used as a control, and C42 > UAS-Lipin[RNAi] and Uro-GAL4 > Lipin[RNAi] were used as experimental groups. No developmental delays were observed (animal lethality was not evaluated due to high standard deviation within biological replicates).



**Figure 11.** Lipin downregulation using C42 and Uro-GAL4 Malpighian tubule drivers does not result in a significant developmental delay compared to controls. After performing a t-test comparing daily pupariation rates, no statistical differences were observed among groups ( $p > 0.05$ ).

Malpighian tubules were stained with Lipin antibody to affirm its nuclear localization in  $w^{1118}$ . The 3<sup>rd</sup> instar larvae were dissected and Lipin protein was labeled in fat body and Malpighian tubules simultaneously. The outcomes of the Lipin staining did not match previous data because Malpighian tubules did not show high Lipin concentration in the nucleus (Figure 12). The difference in the outcomes may potentially arise from the fact that animals from crowded vials were used for the staining that were potentially nutritionally stressed. The nutritional stress these animals experienced



would come from high competition for food as a result of overcrowding. In summary, Lipin staining in Malpighian tubules revealed that there may be a variation in Lipin localization in the nucleus in response to environmental factors.

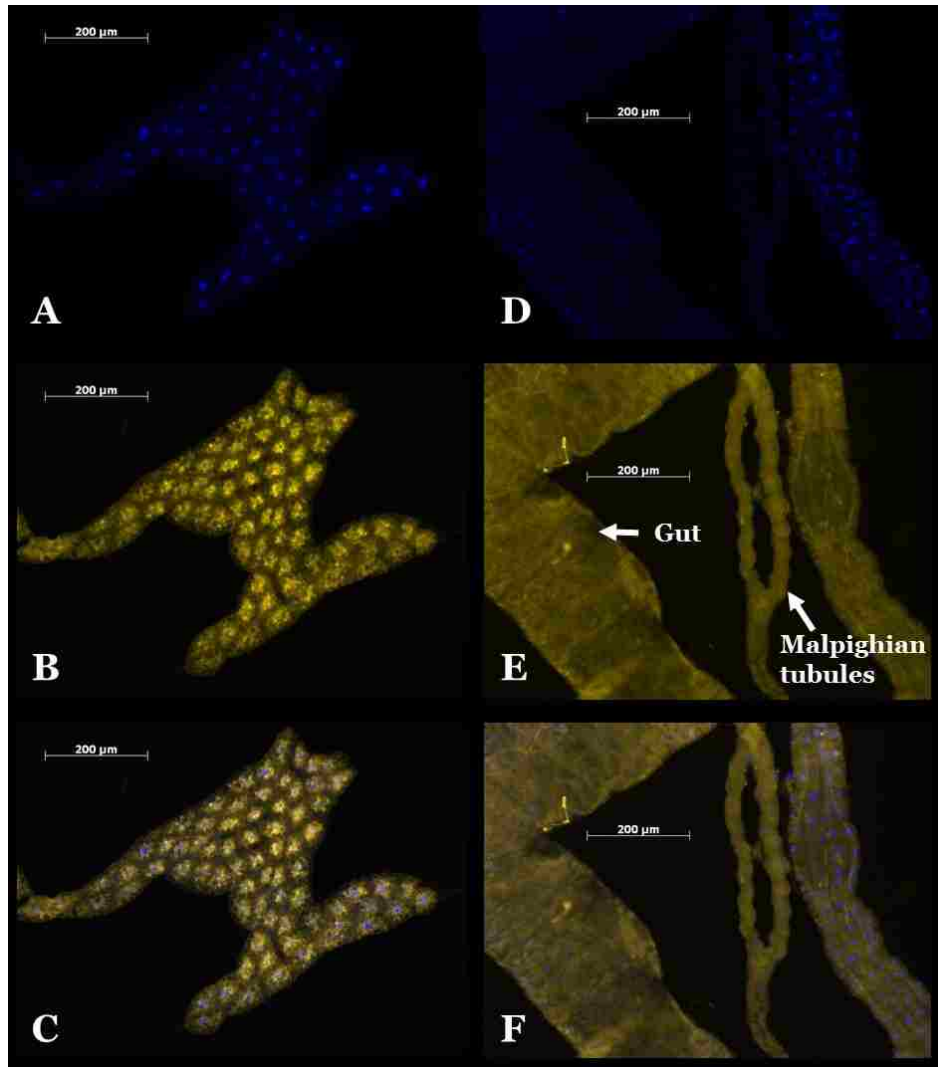


**Figure 12.** Lipin protein staining shows strong cytoplasmic localization in the cells of fat body but not as strong in Malpighian tubules in  $w^{1118}$  (wild-type) animals. (A) and (D) are nuclei labeled with DAPI of fat body and Malpighian tubules respectively. (B) and (E) are Lipin labeled with Cy3. (C) and (F) are image overlaps for DAPI nuclear staining and Cy3 Lipin protein staining. The total magnification used was x100 and exposure of 300 ms.

## **I. Overexpression of Lipin $\Delta$ NLS in the Ring Gland**

Animals that exhibit developmental delay as a result of dominant negative effect of Lipin $\Delta$ NLS can be rescued if fed with 20-hydroxyecdysone (20-E), which is a steroid hormone that determines transitions between larval stages and into an adult (Lehmann lab, unpublished observations). A precursor of 20-E, ecdysone, is produced in the prothoracic gland portion of the ring gland. The ring gland of wild-type animals contains high levels of Lipin protein (Ugrankar et al., 2011). When Lipin $\Delta$ NLS is expressed in ring gland using phmN1 driver, significant developmental delay is observed (M. Lehmann, personal communication). The question addressed in this portion of the thesis is: Will expression of Lipin $\Delta$ NLS using cell type specific drivers for ring gland have a negative effect on animal development?

This question was addressed using the GAL4/UAS system. Two different drivers were used to express either Lipin $\Delta$ NLS or LipinWT in different regions of the ring gland. The first driver was Mai60, which is specific for the prothoracic gland portion of the ring gland. The second driver was Aug21, a driver specific to the corpora allata portion of the ring gland. The significance of using these two drivers is that, as mentioned earlier, prothoracic gland produces ecdysone and corpora allata produces juvenile hormone. The two hormones work together to ensure proper insect development but have fundamentally different functions (Dubrovsky, 2005). Unlike 20-E, juvenile hormone does not initiate transition between the developmental stages but it does function in determining the type of transition that takes place. Lipin $\Delta$ NLS expression in both glands will give us an insight into the functional importance of Lipin's nuclear localization in the ring gland.

Figure 13 shows the outcomes of expressing Lipin $\Delta$ NLS in ring gland using Mai60 and Aug21. The crosses between w<sup>1118</sup> and either UAS-Lipin $\Delta$ NLS, w<sup>1118</sup> and Mai60, or w<sup>1118</sup> and UAS-LipinWT were used as controls. Comparing the four experimental groups, Mai60 > UAS-Lipin $\Delta$ NLS, Aug21 > UAS-Lipin $\Delta$ NLS and Mai60 > UAS-LipinWT, Aug21 > UAS-LipinWT to the control groups, no statistical difference was determined.

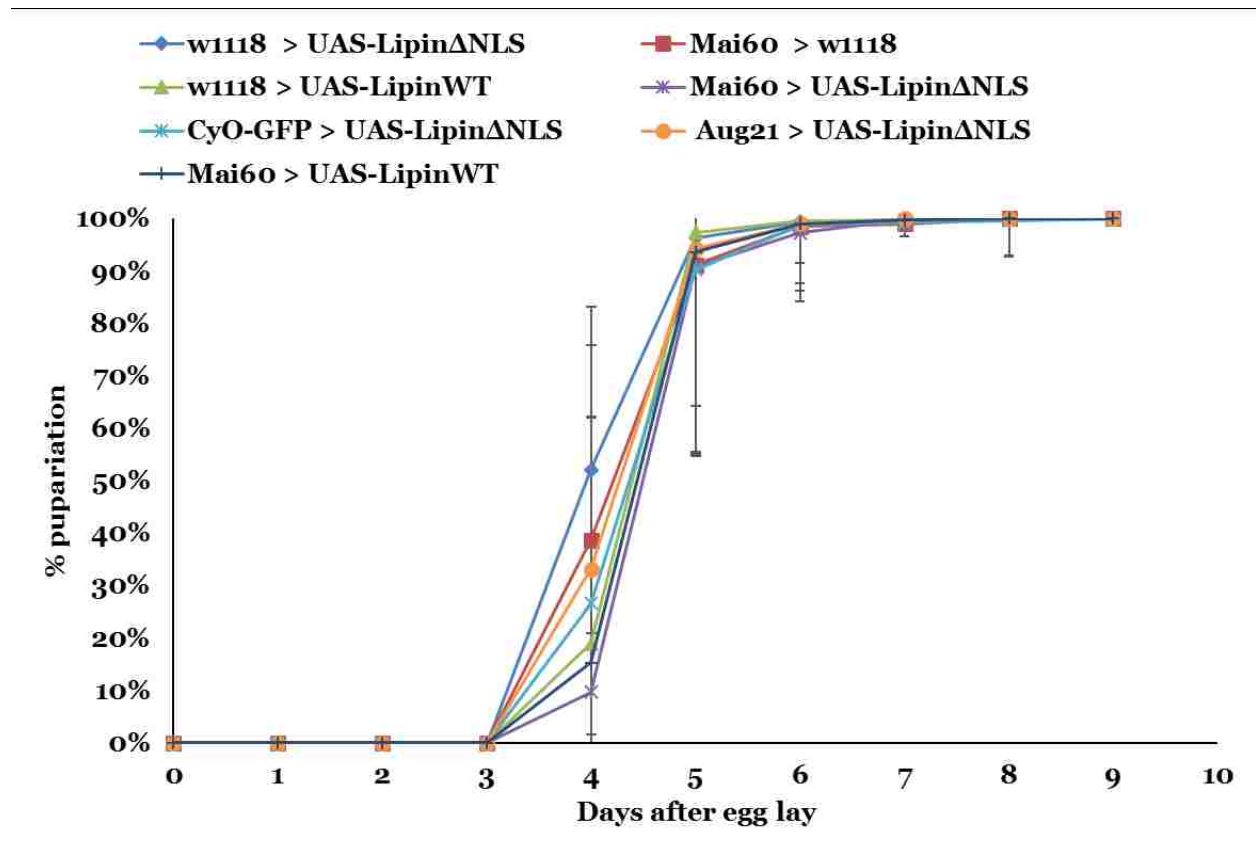


**Figure 13.** Lipin $\Delta$ NLS overexpression in the ring gland using ring gland-specific drivers Mai60 and Aug21. Mai60 driver was used to drive expression in prothoracic gland and Aug21 was used to drive expression in corpora allata. When Lipin $\Delta$ NLS is overexpressed using Mai60, the animals show no significant developmental delay compared to control (unpaired t-test). Overexpression of LipinWT using Mai60 also results in no developmental delay ( $p > 0.05$ ).

#### IV. DISCUSSION

Lipins are proteins found in an array of organisms from *Arabidopsis thaliana* to humans. These proteins participate in controls for fat storage and overall metabolism. Lipins can function as PAPs and as transcriptional co-regulators (Vance et al., 2004). As lipins' role as transcriptional co-regulators is poorly understood, it was the goal of this study to establish the ground work for exploring lipin's interactions with DNA within the nucleus. Lipin proteins have a nuclear localization signal (NLS), which allows their entry into the nucleus where the proteins directly interact with transcription control proteins, which leads to gene activation or repression.

We have generated a *Lipin* $\Delta$ NLS mutant allele by utilizing CRISPR/Cas9 mutagenesis. Our data demonstrates that *Lipin* $\Delta$ NLS is a recessive lethal allele. No animals that are homozygous for the mutation can be observed past the embryo stage. This information suggests the importance of nuclear functions of Lipin for survival.

The *Lipin* $\Delta$ NLS allele was sequenced in order to screen for secondary mutations within the mutagenized *lipin* gene. Eleven primer pairs were used to cover the span of the transcript start site, 5' UTR, all but the first two introns, and all *lipin* exons to the stop codon and including 3' UTR. Three polymorphisms were identified in both alleles of the mutant. These changes were caused by two single nucleotide exchanges causing amino acid changes and an insertion of two nucleotides in 3' UTR. The *Lipin* $\Delta$ NLS allele contained six single nucleotide exchanges within the introns. There were also some other modifications not due to natural polymorphisms. The first modification was the NLS deletion as intended by CRISPR/Cas9 mutagenesis. The next modifications were single nucleotide exchanges in upstream of promoter sequence, 5' UTR, silent

mutations or a single missense mutation in exons, 3' UTR, and downstream of the ORF . This information suggests that outside of NLS, *LipinΔNLS* allele has a few mutations, which are not expected to affect any of the functional Lipin domains but complementation analysis would be needed.

Complementation analysis was conducted using *LipinΔNLS* and *LipinΔPAP* animals. Just like *LipinΔNLS*, *LipinΔPAP* animals can only be heterozygous for the mutant allele. When crossed, we found that the two alleles can complement one another. It already has been shown that mammalian lipin-1 forms homo-oligomers with itself (Guang-Hui et al., 2010). Our suggested mechanism is that *LipinΔNLS* and *LipinΔPAP* can also form an oligomer, which will carry a functional PAP and a functional NLS domain, thus restoring the lost functions to the oligomer. The oligomerization is supported by observed complete rescue of the mutant phenotype.

We were also able to retrieve some unintended mutants generated by CRISPR/Cas9 (See Appendix A for detailed descriptions). The majority of the mutants generated were frame shift mutants caused by deletions or insertions of nucleotides as a result of non-homologous end joining (NHEJ). Three in-frame mutation genotypes including *LipinΔNLS* were retrieved. CRISPR/Cas9 procedure was repeated three times to obtain the desired mutant. In the first run of CRISPR/Cas9 the protospacer did not function as required; there were no mutants present. In the second run, the protospacer directed double-strand breaks by Cas9 took place and a significant number of mutants was generated by NHEJ; however, homology directed repair did not seem to work as no *LipinΔNLS* mutants were recovered. The third run successfully produced a *LipinΔNLS* heterozygous mutant.

The mutants generated by CRISPR/Cas9 were analyzed in the following manner. First, the sequencing results were analyzed based on the type of mutation (frame shift versus in-frame). The mutants were then analyzed for homozygote lethality stage. Next, the mutants were analyzed for secondary site mutations by crossing each of them with flies carrying a deficiency uncovering the *lipin* locus. The results suggest that all but one mutant lack secondary site mutations and cannot produce viable animals when a mutant allele is present over the *lipin* deficiency allele. Finally, Western blot was conducted to evaluate presence of truncated proteins caused by an introduction of a premature stop codon due to frame shift. The fat bodies from 3<sup>rd</sup> instar larvae were dissected and processed to extract total protein. The results of the Western blot were inconclusive due to Lipin protein degradation. For future, a method should be developed to avoid such high rates of degradation.

The importance of nuclear localization of Lipin is well-established in *Drosophila* (Ugrankar et al., 2011). Reduced levels of Lipin affect proper development of fat bodies, in turn, leading to decreased starvation resistance (Ugrankar et al., 2011). However, the effects of Lipin's nuclear localization in different tissues are not well-understood. In this project, we looked at two types of tissues: Malpighian tubules and the ring gland. *Drosophila* larval Malpighian tubules function similar to the kidneys in humans. It was shown by Ugrankar et al. that *w<sup>1118</sup>* animals exhibit strong nuclear localization preference for Lipin (2011). We also know that Lipin $\Delta$ NLS has a dominant negative effect on endogenous Lipin and prevents it from nuclear entry (Schmitt et al., 2015). We first expressed Lipin $\Delta$ NLS using Malpighian tubule-specific driver. The animals were observed for developmental delays. This severe phenotype was not noted as a result of

Lipin $\Delta$ NLS expression. We then expressed Lipin[RNAi] to downregulate the amount of Lipin present in Malpighian tubules alone. There was also no significant effect observed. Analyzing developmental delay as an outcome from manipulating Lipin gene expression in a particular tissue does not reveal effects that are of physiological importance, but do not impact normal development. There may be other impacts of the performed manipulation that would not result in a developmental delay. The primary function of Malpighian tubules is excretory and osmoregulatory (Nicholls 1985). The effect of low Lipin level or lack of Lipin's nuclear localization may be more noticeable if Malpighian tubules are observed under stress conditions. Their ability to retain water in dry conditions, as well as rate of waste secretion or urine formation can be evaluated (Nicholls 1985). More experimental work would have to be completed to assess the mechanism of Lipin's nuclear function in Malpighian tubules in the future.

The second tissue that was tested for the importance of Lipin's nuclear localization was the ring gland. The effects of Lipin $\Delta$ NLS expression in prothoracic gland and corpora allata were evaluated. We were not able to observe any developmental delays for animals that expressed Lipin $\Delta$ NLS in either of the cases. Our laboratory previously showed an effect of Lipin $\Delta$ NLS expression in prothoracic gland on larval development using the ring gland-specific phmN1 GAL4 driver (Unpublished data). It is known from the literature that there is a significant variation in the strength of the drivers (Pfeiffer et al., 2010). In other words, not all drivers that are either ubiquitous or tissue-specific will result in equal rates of target gene transcription. It is likely that the strength of the drivers used in this project was not sufficient to cause a developmental delay.

In conclusion, this project was able to achieve the primary goal of generating and identifying a *Lipin $\Delta$ NLS* mutant. We were not able to generate a stock that would be homozygous for the *Lipin $\Delta$ NLS* allele. We can conclude that nuclear localization of Lipin is essential for animal survival. Possession of this mutant line opens a number of possibilities for future research. For example, tissue specific drivers can now be used in *Lipin $\Delta$ NLS* background to express Lipin<sup>WT</sup> or Lipin $\Delta$ PAP that carry a functional NLS. These types of rescue experiments will help identify the tissues where nuclear localization of Lipin is essential for animal's development. Although we were unable to observe significant effects of expressing Lipin $\Delta$ NLS transgene in Malpighian tubules or in the ring gland by our chosen methodology and evaluation criteria, the generation of a Lipin $\Delta$ NLS mutant provides a variety of future directions that can be pursued by our laboratory.

## V. REFERENCES

- Chatterjee D, Katewa SD, Qi Y, Jackson SA, Kapahi P, Jasper H. (2014). Control of metabolic adaptation to fasting by dILP6-induced insulin signaling in *Drosophila* oenocytes. *Proc Natl Acad Sci U S A.*;111(50):17959-64.
- Chen Z, Gropler MS, Norris J, et al. (2008). Alternations in hepatic metabolism in *fld* mice reveal a role of lipin-1 in regulating VLDL-triacylglyceride secretion. *Arterioscler Thromb Vsc Biol* 28:1738-1744.
- DiAngelo, JR and Birnbaum, MJ.(2009). Regulation of fat cell mass by insulin in *Drosophila melanogaster*. *Mol. Cell. Biol.* 29, 6341–6352.
- Donkor J, Sariahmetoglu M, Dewald J, et al. (2007). Three mammalian lipins act as phosphatidate phosphatases with distinct tissue expression patterns. *J Biol Chem* 282:3450-3457.
- Dubrovsky EB. Hormonal cross talk in insect development. (2005). *Trends in Endocrinology and Metabolism* 16(1):6-11.
- Echalier G. (1997). *Drosophila* Cells in Culture, Academic Press, San Diego.10.



- Echalier G. and Ohanessian, A. (1969). Isolation, in tissue culture, of *Drosophila melanogaster* cell lines. C. R. Acad. Sci. Hebd. Seances Acad. Sci. D. 268, 1771–1773.
- El-Shanti HI, Ferguson PJ. (2007). Chronic recurrent multifocal osteomyelitis: a concise review and genetic update. Clin Orthop Relat Res 462:11-19.
- Ferguson PJ, Chen S, Teyeh MK, et al. (2005). Homozygous mutations in *LPIN2* are responsible for the syndrome of chronic recurrent multifocal osteomyelitis and congenital dyserythropoetic anaemia (Majeed syndrome). J Med Genet 42:551-557.
- Finck BN, Gropler MC, Chen Z, Leone TC, Croce MA, Harris TE, Lawrence Jr. JC, and Kelly DP. (2006). Insulin controls subcellular localization and multisite phosphorylation of the phosphatidic acid phosphatase, lipin 1. J Biol Chem 282, 277-286.
- Finck\* BN, Gropler MC, Chen Z, et al. (2006). Lipin 1 is an inducible amplifier of the hepatic PGC-1alphaPPARalpha regulatory pathway. Cell Metab 4:199-210.
- Garg A. Acquired and inherited lipodystrophies. (2004). N Engl J Med 350, 1220-1234.
- Green C. J., Pramfalk C., Morten K. J. and Hodson L. (2015). From whole body to cellular models of hepatic triglyceride metabolism: man has got to know his limitations. Am. J. Physiol. Endocrinol. Metab. 308, E1-E20.
- Guang-Hui L, Qu J, Carmack AE, Kim HB, Chen C, Ren H, Morris AJ, Finck BN, and Harris TE. (2010). Lipin proteins form homo- and hetero-oligomers. Biochem J. 432(1): 65–76.
- Gutierrez E, Wiggins D, Fielding B, Gould AP. (2007). Specialized hepatocyte-like cells regulate *Drosophila* lipid metabolism. Nature 445(7125): 275-280.
- Hans GS, Wu WI, Carman GM. (2006). The *Saccharomyces cerevisiae* lipin homolog is a Mg<sup>2+</sup> dependent phosphatidate phosphatase enzyme. J Biol Chem 281:9210-9218.
- Harris, T E and Finck, B N. (2011). Dual function lipin proteins and glycerolipid metabolism. Trends Endocrinol. Metab. 22, 226–233.
- Harris TE, Huffman TA, Chi A, et al. (2007). Insulin controls subcellular localization and multisite phosphorylation of the phosphatidic acid phosphatase, lipin 1. J Biol Chem 282:277-286.
- Huffman TA, Mothe-Satney I, Lawrence JC Jr. (2002). Insulin-stimulated phosphorylation of lipin mediated by the mammalian target of rapamycin. Proc Natl Acad Sci USA 99, 1047-1052.
- Kim SK, and Rulifson EJ. (2004). Conserved mechanisms of glucose sensing and regulation by *Drosophila* corpora cardiaca cells. Nature 431:316-320.

- Kim Y, Gentry MS, Harris TE, et al. (2007). A conserved phosphatase cascade that regulated nuclear membrane biogenesis. *Proc Natl Acad USA* 104:6596-6601.
- Kuhnlein RP. (2011). The contribution of the *Drosophila* model to lipid droplet research. *Prog Lipid Res* 50:348-356.
- Langer CA, Birkenmeier EH, Ben-Zeev O, et al. (1989). The fatty liver dystrophy (*fld*) mutation. A new mutant mouse with a developmental abnormality in triglyceride metabolism and associated tissue-specific defects in lipoprotein lipase and hepatic lipase activities. *J Biol Chem* 264:7994-8003.
- Majeed HA, Al-Tarawna M, El-Shanti H, et al. (2001). The syndrome of chronic recurrent multifocal osteomyelitis and congenital dyserythropoetic anaemia. Report of a new family and a review. *Eur J Pediatr* 160:705-710.
- Milhavet F, Cuisset L, Hoffman HM, et al. (2008). The inverse autoinflammatory mutation online registry: update with new genes and functions. *Hum Mutat* 19:803-808.
- Murphy DJ. (2012). The dynamic roles of intracellular lipid droplets: from Archaea to mammals. *Protoplasma* 249:541-585.
- Nadra K, de Preux CSA, Medar JJ, et al. (2008). Phosphatidic acid mediates demyelination in *Lpin1* mutant mice. *Genes Dev* 22:1647-1661.
- Nicholls SP. (1985). Fluid secretion by the Malpighian tubules of dragonfly *Libellula quadrimaculata*. Printed in Great Britain © The Company of Biologists Limited.
- Péterfy M, Phan J, Xu P, and Reue K. (2001). Lipodystrophy in the *fld* mouse results from mutation of a new gene encoding a nuclear protein, lipin. *Nat Genet* 27, 121-124.
- Péterfy M, Harris TE, Fujita N and Reue K. (2010). Insulin-stimulated interaction with 14-3-3 promotes cytoplasmic localization of lipin-1 in adipocytes. *J. Biol. Chem.* 285, 3857-3864.
- Petersen, UM, Kadalayil L, Rehorn KP, Hoshizaki DK, Reuter R and Engstrom Y. (1999). Serpent regulates *Drosophila* immunity genes in the larval fat body through an essential GATA motif. *EMBO J.* 18, 4013-4022.
- Pfeiffer BD, Ngo T-TB, Hibbard KL, et al. (2010). Refinement of Tools for Targeted Gene Expression in *Drosophila*. *Genetics* 186(2):735-755.
- Phan J and Reue K. (2005). Lipin, lipodystrophy and obesity gene. *Cell Metab* 1, 73-83.
- Phan J, Péterfy M, Rue K. (2004). Lipin expression preceding peroxisome-proliferator activated receptor gamma is critical for adipogenesis *in vivo* and *in vitro*. *J Biol Chem* 279:29558-295664.

- Port F, Chen HM, Lee T, Bullock SL. (2014). Optimized CRISPR/Cas tools for efficient germline and somatic genome engineering in *Drosophila*. Proc Natl Acad Sci U S A. 111(29):E2967-76.
- Richardson CD, Ray GJ, DeWitt MA, Curie GL, Corn JE. (2016). Enhancing homology-directed genome editing by catalytically active and inactive CRISPR-Cas9 using asymmetric donor DNA. Nature Biotechnology 34, 339–344.
- Rulifson EJ, Kim SK and Nusse R. (2002). Ablation of insulin-producing neurons in flies: growth and diabetic phenotypes. Science 296, 1118–1120.
- Saltiel AR and Kahn CR. (2001). Insulin signaling and the regulation of glucose and
- Santos-Rosa H, Leung J, Grimsey N, Peak-Chew S, and Siniossoglou S. (2005). The yeast lipin Smp2 couples phospholipid biosynthesis to nuclear membrane growth. EMBO J 24, 1931-1941.
- Schmitt S, Ugrankar R, Greene SE, Prajapati M, and Lehmann M. (2015). *Drosophila* Lipin interacts with insulin and TOR signaling pathways in the control of growth and lipid metabolism. J Cell Sci. 128(23):4395-406.
- Sirvent P, Mercier J, Lacampagne A. (2008). New insights into mechanisms of statin-associated myotoxicity. Curr Opin Pharmacol 8:333-338.
- Smyth S and Heron A. (2006). Diabetes and obesity: the twin epidemics. Nat Med 12, 75-80.
- Ugrankar R, Liu Y, Provaznik J, Schmitt S, and Lehmann M. (2011). Lipin is a central regulator of adipose tissue development and function in *Drosophila melanogaster*. J Cell Biol 1, 1646-1656.
- Vance JE and Vance DE. (2004). Phospholipid biosynthesis in mammalian cell. Biochem Cell Biol 82, 113-128.
- Wullschleger S, Loewith R and Hall MN. (2006). TOR Signaling in Growth and Metabolism. Cell 124, 471–484.
- Zechner R, Strauss JG, Haemmerle G, Lass A and Zimmermann R. (2005). Lipolysis: pathway under construction. Curr. Opin. Lipidol. 16, 333-340.
- Zeharia A, Shaag A, Houtkooper RH, et al. (2008). Mutations in *LPIN1* cause recurrent acute myoglobinuria in childhood. Am J Hum Genet 83:1-6.

**VI. APPENDIX: NUCLEOTIDE AND AMINO ACID ALIGNMENTS OF CRISPR/CAS GENERATED MUTANTS**

**A. LipinNLS+6(+2)FS285**

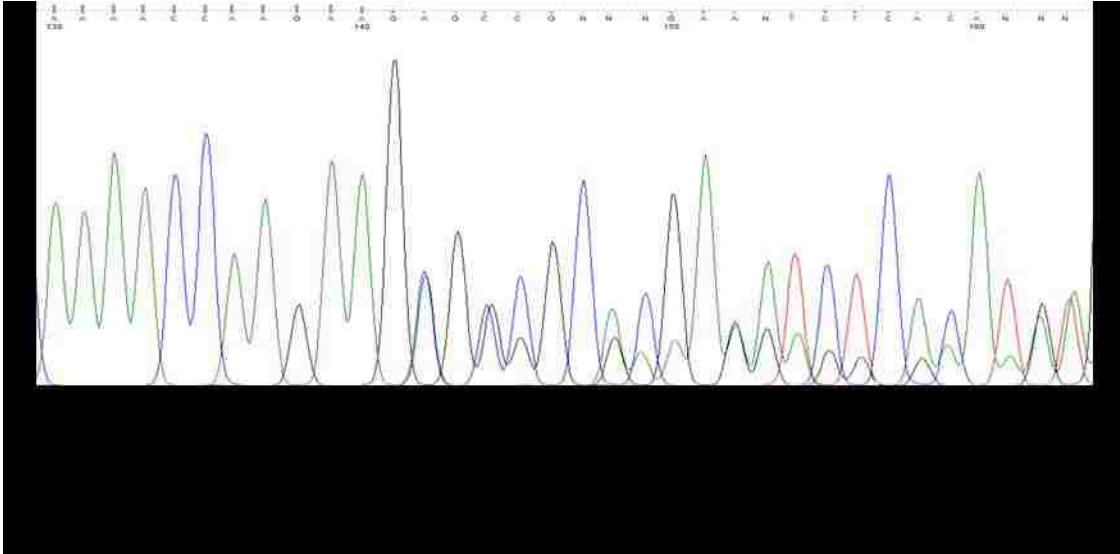


**Figure 14.** FS277 CRISPR mutagenized animal. This frame shift animal genotype has a two nucleotide insertion AG, which results in premature stop codon at position 285.

Modified protein derived from the mutagenized *Lipin* allele:

```
MNSLARVFSNFRDFYNDINAATLTGAIDVIVVEQRDGEFQCSPFHVRFGK
LGVLSREKVVDIEINGVPVDIQMKLGDSGEAFFVEECLEDEDEELPANL
ATSPIPNSFLASRDKANDTMEDISGVVTDKNASELLLPLPLPRRNSIDF
SKEEPKEAVVEGSKFENQVSDYTQRRHTDNTLERRNLSEKLKEFTTQKIR
QEWAHEEELFQGEKKPADSDSLDNQSKASNEAETEKAIPIAVIEDTEKEKD
QIKPDVNLT VTTSEATKEVSKSKTKKSGARSRK Stop
```

## B. LipinNLS\_IF276ΔK

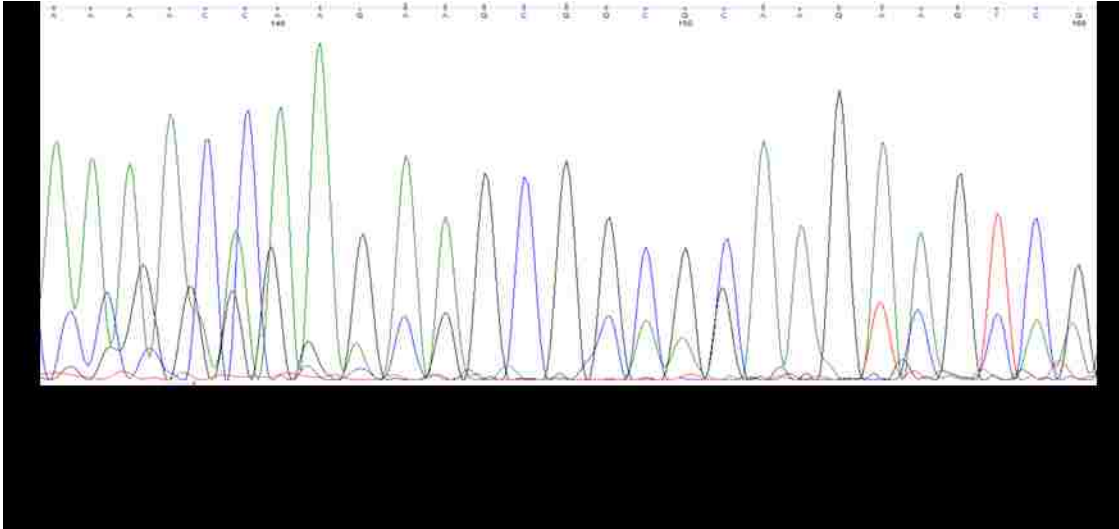


**Figure 15.** IF276 CRISPR mutagenized animal. This in-frame mutation animal genotype lack AAG or K as a part of the start of NLS sequence.

Modified protein derived from the mutagenized *Lipin* allele:

```
MNSLARVFSNFRDFYNDINAATLTGAIDVIVVEQRDGEFQCSPFHVRF GK
LGV LRSREKVV DIEINGVPVDIQMKLGDSGEAFFVEECLEDEDEELPANL
ATSPIPNSFLASRDKANDTMEDISGVVTDKNASEELLLPLPLPRRNSIDF
SKEEPKEAVVEGSKFENQVSDYTQRRHTDNTLERRNLSEKLKEFTTQKIR
QEWAEHEELFQGEKKPADSDSLDNQSKASNEAETEKAI PAVIEDTEKEKD
QIKPDVNLTTVTTSEATKEVSKSKTKΔRRKKSQMKNNAQRKNSSSSSLGS
AGGGDLPSAETPSLGVSNI DEGDAPISSATNNNNNTSSSNDEQLSAPLVTA
RTGDDSP LSEIPH TPTSNPRLDLDIHFFSDTEITTPVGGGGAGSGRAAGG
RPSTPIQSDSELETTMRDNRHV VTEESTASWKWGELPTPEQAKNEAMSA A
QVQQSEHQSM LSNMFSFMKRANRLRKEKGVGEVGD IYLSDL DAGSMDPEM
AALYFPSPLSKAASPPEEDGESGNGTSLPHSPSSLEEGQKSIDSDFDETK
QQRDNNRYLDFVAMSMCGMSEQ GAPPSDEEFDRHLVNYPDVCKSPSIFSS
PNLVVRLNGKY YTWMAACPIVMTMITFQKPLTHDAIEQLMSQTVDGKCLP
GDEKQEAVAQADNGGQTKRYWWSWRRSQDAAPNHLNNT HGMPLGKDEKDG
DQAAVATQTSRPTSPDITDPTLSKSDSLVNAENTSALVDNLEELTMASNK
SDEPKERYK KSLRLSSAAIKKLN LKEGMNEIEFSVTTAYQGTT RCKCYLF
RWKHNDKVVISDIDGTITKSDV LGHILPMVGKDWAQLGVAQLFSKIEQNG
```

YKLLYLSARAIGQSRVTREYLRSIRQGNVMLPDGPLLLNPTSLISAFHRE  
 VIEKKPEQFKIACLSDIRDLFPDKEPFYAGYGNRINDVWAYRAVGIPIMR  
 IFTINTKGELKHELTQTFQSSGYINQSLEVDEYFPLLTNQDEFDYRTDIF  
 DDEESEELQFSDDYDVDVEHGSSEESSGDEDDDEALYNDDFANDDNGIQ  
 AVVASGDERTADVGLIMRVRRVSTKNEVIMASPPKWINS

**C. LipinNLS\_IF273ΔKTK**

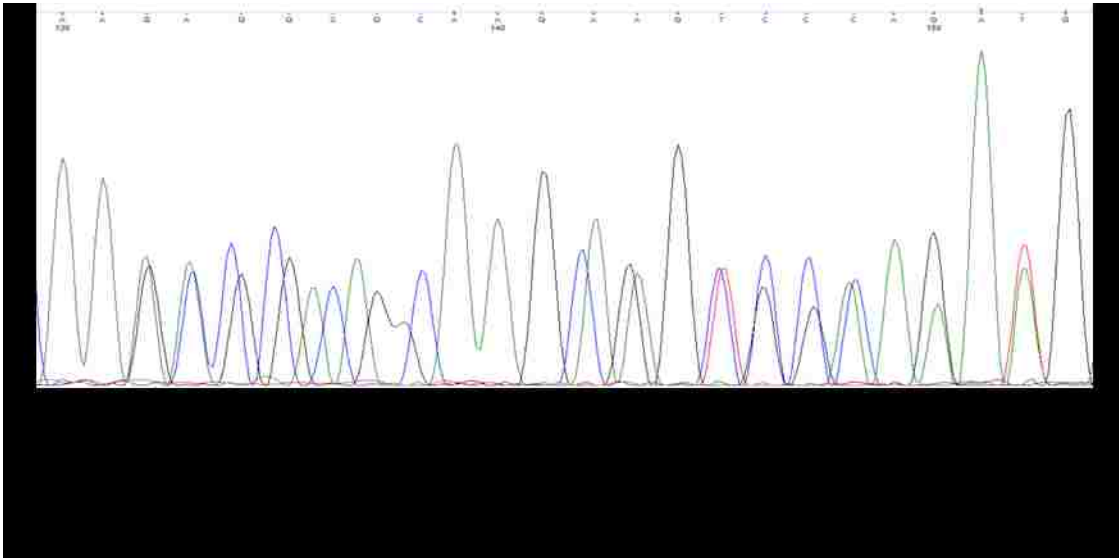


**Figure 16.** IF273 CRISPR mutagenized animal. This in-frame mutation animal genotype lack AAAACCAAG or KTK as a part of the start of NLS sequence.

Modified protein derived from the mutagenized *Lipin* allele:

MNSLARVFSNFRDFYNDINAATLTGAIDVIVVEQRDGEFQCSPFHVRF GK  
 LGVLSREKVVDIEINGVPVDIQMKLGDSGEAFFVEECLEDEDEELPANL  
 ATSPIPNSFLASRDKANDTMEDISGVVTDKNASEELLPLPLPRRNSIDF  
 SKEEPKEAVVEGSKFENQVSDYTQRRHTDNTLERRNLSEKLKEFTTQKIR  
 QEWAHEELFQGEKKPADSDSLDNQSKASNEAETEKAIPAVIEDTEKEKD  
 QIKPDVNLTVTTSEATKEVSKSΔKRRKKSQMKNNAQRKNSSSSSLGS  
 AGGGDLPSAETPSLGVSNI DEGDAPISSATNNNNTSSSNDEQLSAPLVTA  
 RTGDDSPLEIPHTPTSNPRLDLIHFFSDTEITTPVGGGGAGSGRAAGG  
 RPSTPIQSDSELETTMRDNRHVVTEESTASWKWGELPTPEQAKNEAMSAA  
 QVQQSEHQSMLSNMFSFMKRANRLRKEKGVGEVVDIYLSDL DAGSMDPEM  
 AALYFPSPLSKAASPPEEDGESGNGTSLPHSPSSLEEGQKSIDSDFDETK

QQRDNNRYLDFVAMSMCGMSEQGAPPSDEEFDRHLVNYPDVCKSPSIFSS  
 PNLVVRLNGKYITWMAACPIVMTMITFQKPLTHDAIEQLMSQTVDGKCLP  
 GDEKQEAVAQADNGGQTKRYWWSWRRSQDAAPNHLNNTHGMPGKDEKDG  
 DQAAVATQTSRPTSPDITDPTLSKSDSLVNAENTSALVDNLEELTMASNK  
 SDEPKERYKKSRLSSAAIKKLNKEGMNEIEFSVTTAYQGTTRCKCYLF  
 RWKHNDKVVISDIDGTITKSDVLGHILPMVGKDWAQLGVAQLFSKIEQNG  
 YKLLYLSARAIGQSRVTREYLR SIRQGNVMLPDGPLLLNPTSLISAFHRE  
 VIEKKPEQFKIACLSDIRDLFPDKEPFYAGYGNRINDVWAYRAVGIPIMR  
 IFTINTKGELKHELTQTFQSSGYINQSLEVDEYFPLLTNQDEFDYRTDIF  
 DDEESEELQFSDDYDVDVEHGSSEESSGDEDDDEALYNDDFANDDNGIQ  
 AVVASGDERTADVGLIMRVRVSTKNEVIMASPPKWINS

**D. LipinNLS $\Delta$ 1FS284**

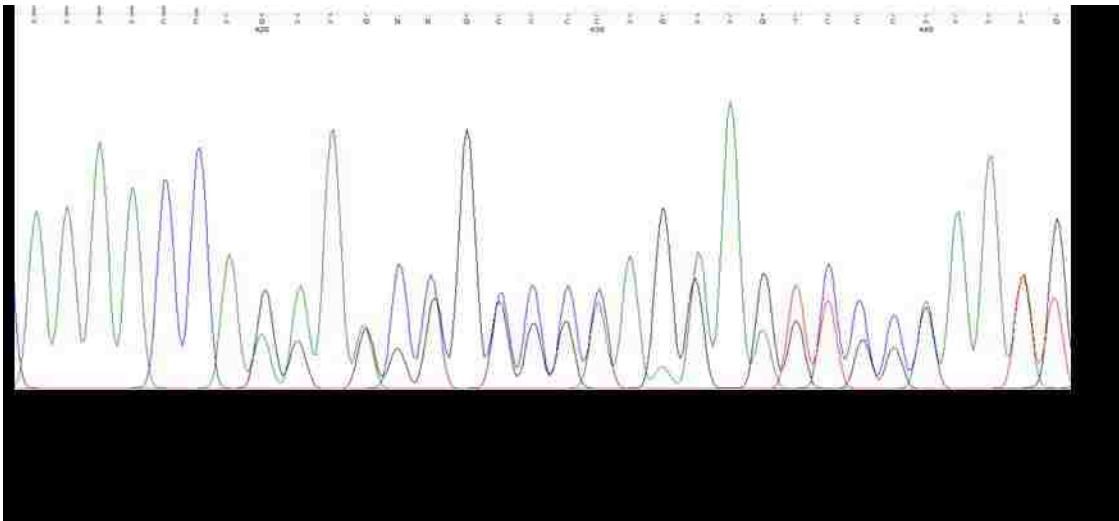


**Figure 17.** FS275 CRISPR mutagenized animal. This frame shift animal genotype has a one nucleotide deletion A, which results in premature stop codon at position 284.

Modified protein derived from the mutagenized *Lipin* allele:

MNSLARVFSNFRDFYNDINAATLTGAIDVIVVEQRDGEFQCSPFHVRFGK  
 LGVLSREKVV DIEINGVPVDIQMKLGDSGEAFFVEECL EDEDEELPANL  
 ATSPIPNSFLASRDKANDTMEDISGVVTDKNASELLLLPLPLPRRNSIDF  
 SKEEPKEAVVEGSKFENQVSDYTQRRHTDNTLERRNLSEKLKEFTTQKIR  
 QEWAHEELFQGEKKPADSDSLDNQSKASNEAETEKAIPAVIEDTEKEKD

QIKPDVNLTTVTTSEATKEVSKSKTRSGARSRK **Stop**

**E. LipinNLS+2Δ1FS284**

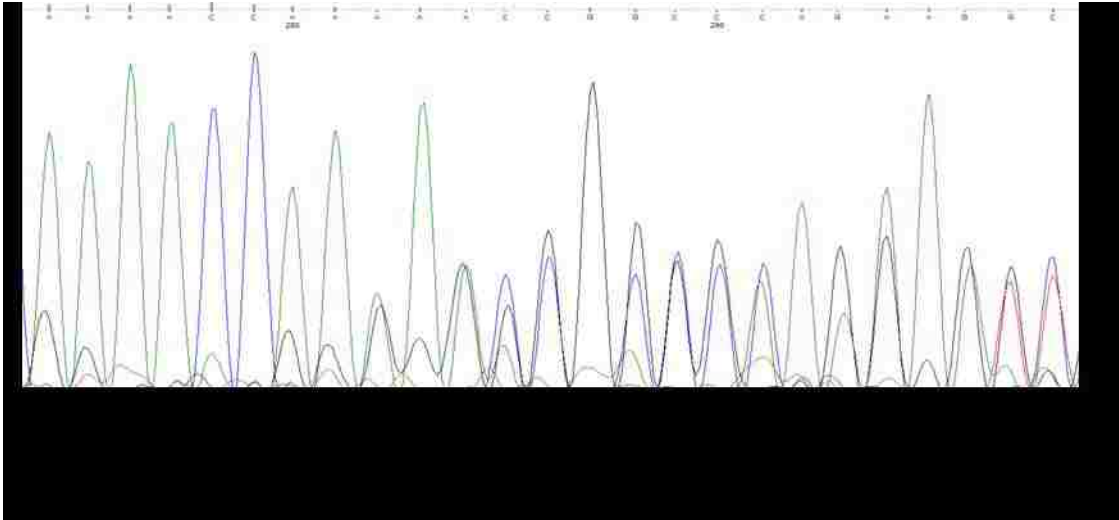


**Figure 18.** FS275 CRISPR mutagenized animal. This frame shift animal genotype has a one nucleotide deletion at the beginning of the NLS sequence, G, which results in premature stop codon at position 284.

Modified protein derived from the mutagenized *Lipin* allele:

MNSLARVFSNFRDFYNDINAATLTGAIDVIVVEQRDGEFQCSPFHVRFGK  
LGVLSREKVVDIEINGVPVDIQMKLGDSGEAFVVEECLEDEDEELPANL  
ATSPIPNSFLASRDKANDTMEDISGVVTDKNASELLLPLPLPRRNSIDF  
SKEEPKEAVVEGSKFENQVSDYTQRRHTDNTLERRNLSEKLKEFTTQKIR  
QEWAEHEELFQGEKKPADSDSLDNQSKASNEAETEKAIPAVIEDTEKEKD  
QIKPDVNLTTVTTSEATKEVSKSKTRSGARSRK **Stop**



## F. LipinNLS $\Delta$ 2FS304

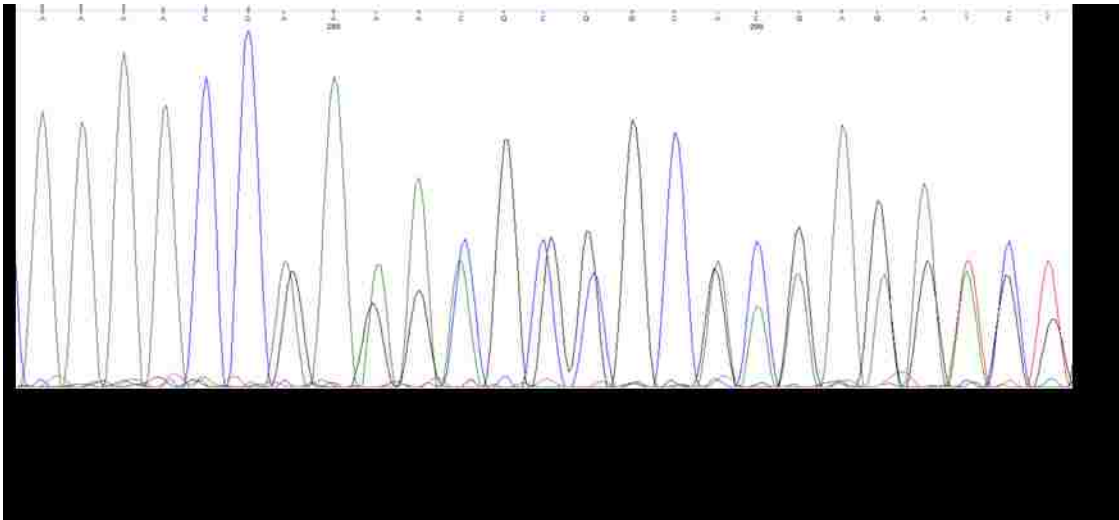


**Figure 19.** FS275 CRISPR mutagenized animal. This frame shift animal genotype has a two nucleotide deletion at the beginning of the NLS sequence, AA, which results in premature stop codon at position 304.

Modified protein derived from the mutagenized *Lipin* allele:

```
MNSLARVFSNFRDFYNDINAATLTGAIDVIVVEQRDGEFQCSPFHVRF GK
LGV LRSREKVVDIEINGVPVDIQMKLGDSGEAFFVEECLEDEDEELPANL
ATSPIPNSFLASRDKANDTMEDISGVVTDKNASELLLLPLPLPRRNSIDF
SKEEPKEAVVEGSKFENQVSDYTQRRHTDNTLERRNLSEKLKEFTTQKIR
QEWAEHEELFQGEKKPADSDSLDNQSKASNEAETEKAI PAVIEDTEKEKD
QIKPDVNLTTVTTSEATKEVSKSKTEAAQEVA NEEECPAQELFKQLIGQRRRR
Stop
```

### G. LipinNLS+2Δ5FS303

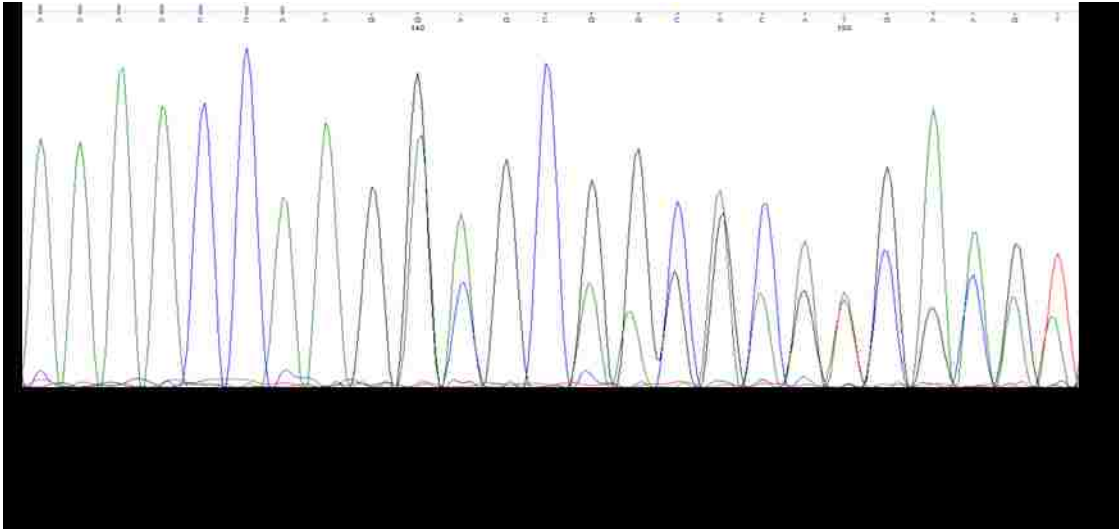


**Figure 20.** FS276 CRISPR mutagenized animal. This frame shift animal genotype has a five nucleotide deletion at the beginning of the NLS sequence, GAAGC, which results in premature stop codon at position 303.

Modified protein derived from the mutagenized *Lipin* allele:

```
MNSLARVFSNFRDFYNDINAATLTGAIDVIVVEQRDGEFQCSPFHVRF GK
LGV LRSREKVVDIEINGVPVDIQMKLGDSGEAFFVEECLEDEDEELPANL
ATSPIPNSFLASRDKANDTMEDISGVVTDKNASELLLLPLPLPRRNSIDF
SKEEPKEAVVEGSKFENQVSDYTQRRHTDNTLERRNLSEKLKEFTTQKIR
QEWAEHEELFQGEKKPADSDSLDNQSKASNEAETEKAI PAVIEDTEKEKD
QIKPDVNLTTVTTSEATKEVSKSKTKAQEVANEEECPAQELFKQLIGQRRR
Stop
```

## H. LipinNLS $\Delta$ 5FS303

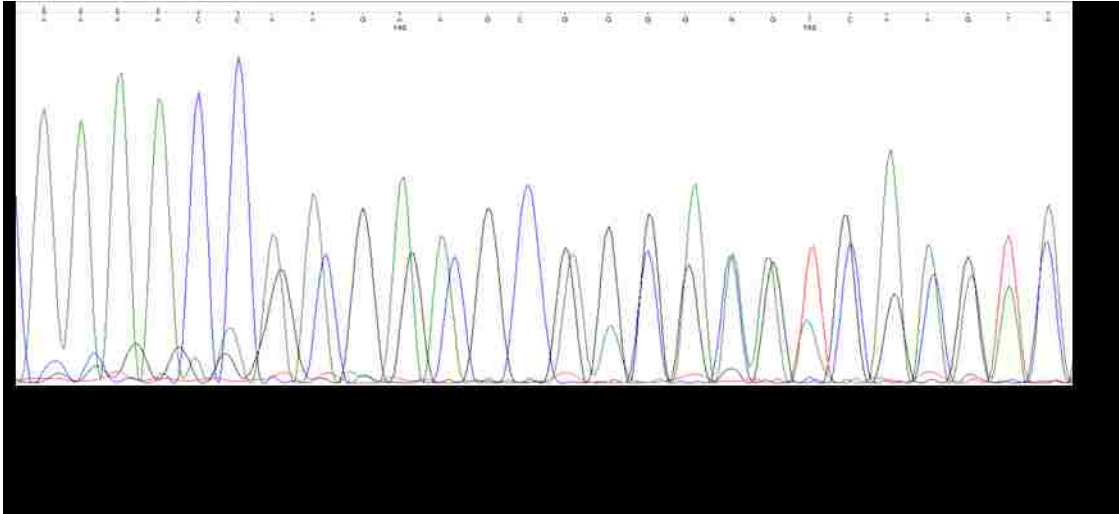


**Figure 21.** FS275 CRISPR mutagenized animal. This is a frame shift mutation and the animal has genotype that lacks five nucleotides, AAGAA, at the beginning of NLS sequence results in premature stop codon at position 303.

Modified protein derived from the mutagenized *Lipin* allele:

```
MNSLARVFSNFRDFYNDINAATLTGAIDVIVVEQRDGEFQCSPFHVRFGK
LGVLSREKVVVDIEINGVPVDIQMKLGDSGEAFFVEECLEDEDEELPANL
ATSPIPNSFLASRDKANDTMEDISGVVTDKNASELLLLPLPLPRRNSIDF
SKEEPKEAVVEGSKFENQVSDYTQRRHTDNTLERRNLSEKLKEFTTQKIR
QEWAHEELFQGEKKPADSDSLDNQSKASNEAETEKAIPAVIEDTEKEKD
QIKPDVNLTTVTTSEATKEVSKSKTAAQEVANEEECPAQELFKQLIGQRRR
Stop
```

## I. LipinNLS-3Δ7FS282

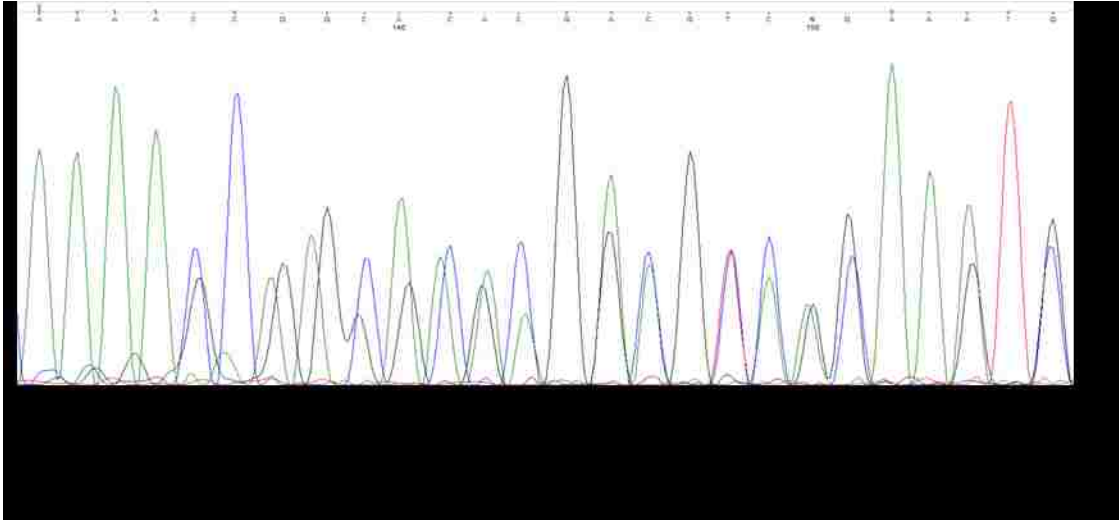


**Figure 22.** FS274 CRISPR mutagenized animal. This frame shift animal genotype has a seven nucleotide deletion ACCAAGA, which results in premature stop codon at position 282.

Modified protein derived from the mutagenized *Lipin* allele:

MNSLARVFSNFRDFYNDINAATLTGAIDVIVVEQRDGEFQCSPFHVRFGK  
LGVLSREKVVVDIEINGVPVDIQMKLGDSGEAFFVEECLEDEDEELPANL  
ATSPIPNSFLASRDKANDTMEDISGVVTDKNASELLLLPLPLPRRNSIDF  
SKEEPKEAVVEGSKFENQVSDYTQRRHTDNTLERRNLSEKLKEFTTQKIR  
QEWAEHEELFQGEKKPADSDSLDNQSKASNEAETEKAIPAVIEDTEKEKD  
QIKPDVNLTTVTTSEATKEVSKSKSGARSRK **Stop**

## J. LipinNLS-6Δ13FS280

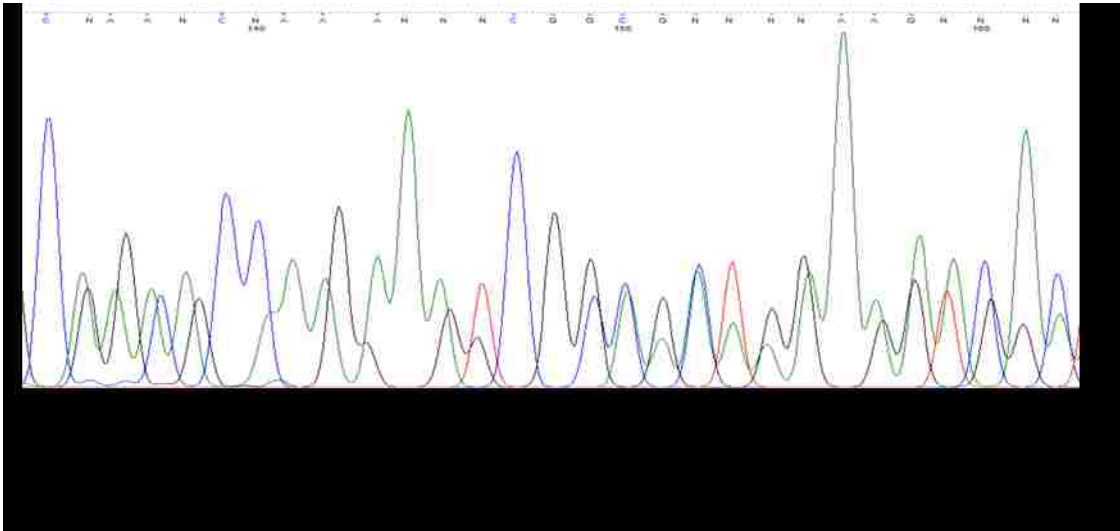


**Figure 23.** FS273 CRISPR mutagenized animal. This frame shift animal genotype has a 13 nucleotide deletion AAAACAAGAAGC, which results in premature stop codon at position 280.

Modified protein derived from the mutagenized *Lipin* allele:

MNSLARVFSNFRDFYNDINAATLTGAIDVIVVEQRDGEFQCSPFHVRF GK  
LGV LRSREKVVDIEINGVPVDIQMKLGDSGEAFFVEECLEDEDEELPANL  
ATSPIPNSFLASRDKANDTMEDISGVVTDKNASEELLPLPLPRRNSIDF  
SKEEPKEAVVEGSKFENQVSDYTQRRHTDNTLERRNLSEKLKEFTTQKIR  
QEWAEHEELFQGEKKPADSDSLDNQSKASNEAETEKAIPAVIEDTEKEKD  
QIKPDVNLTVTTSEATKEVSKSGARSRK **Stop**

### K. LipinNLS-47Δ47(+1)FS269

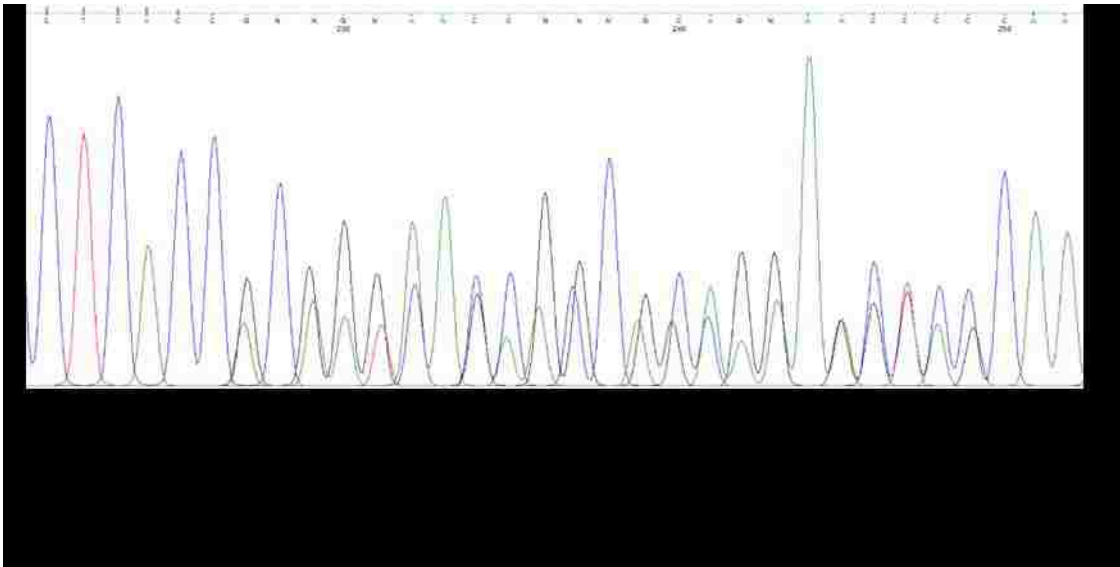


**Figure 24.** FS259 CRISPR mutagenized animal. This frame shift animal genotype has a 47 nucleotide deletion ACGGTCACAACCAGCGAAGCCACCAAGGAGGTGTCCAAGAGCAAAC, and either a point mutation which introduces G instead of the first A in the deleted sequence, or, more likely, an insertion of a G at the cut site, which results in premature stop codon at position 269.

Modified protein derived from the mutagenized *Lipin* allele:

```
MNSLARVFSNFRDFYNDINAATLTGAIDVIVVEQRDGEFQCSPFHVRF GK
LGV LRSREKVVDIEINGVPVDIQMKLGDSGEAFFVEE CLEDEDEELPANL
ATSPIPNSFLASRDKANDTMEDISGVVTDKNASE ELLLPLPLPRRNSIDF
SKEEPKEAVVEGSKFENQVSDYTQRRHTDNTLERRNLSEKLKEFTTQKIR
QEWAEHEELFQGEKKPADSDSLDNQSKASNEAET EKAIPAVIEDTEKEKD
QIKPDVNLTARSGARSRK Stop
```